Title: A New Elpistostegalian from the Late Devonian of the Canadian Arctic and the diversity of stem tetrapods

Authors: T.A. Stewart[1]*, J.B. Lemberg[1]*, A. Daly[1], E.B. Daeschler[2], N.H. Shubin[1†]

Affiliations:

[1]Department of Organismal Biology and Anatomy, University of Chicago; Chicago, USA.

[2]Department of Vertebrate Zoology, Academy of Natural Sciences of Drexel University, Philadelphia, USA.

*These authors contributed equally. Order determined by coin toss.

[†]Corresponding author. Email: nshubin@uchicago.edu

A fundamental gap in the study of the origin of limbed vertebrates lies in understanding the morphological and functional diversity of their closest relatives. While analyses of the elpistostegalians *Panderichthys rhombolepis*, *Tiktaalik roseae* and *Elpistostege watsoni* have revealed a sequence of changes in locomotor, feeding and respiratory structures during the transition[1-9], an isolated bone, a putative humerus, has controversially hinted at a wider range in form and function than currently recognized[10-14]. Here we report the discovery of a new elpistostegalian from the Late Devonian of the Canadian Arctic that reveals surprising disparity in the group. The specimen includes partial upper and lower jaws, pharyngeal elements, a pectoral fin, and scalation. This new genus is phylogenetically proximate to *T. roseae* and *E. watsoni* but evinces significant differences from both taxa and, indeed, other described tetrapodomorphs. Lacking processes, joint orientations, and muscle scars indicative of appendage-based support on a hard substrate[13], its pectoral fin shows specializations for swimming that are unlike those known from other sarcopterygians. This unexpected morphological and functional diversity represents a previously hidden ecological expansion, a secondary return to open water, near the origin of limbed vertebrates.

Study of tetrapodomorph skulls, fins, axial skeleton, and scalation has revealed the ways that feeding, respiration, and appendage-based locomotion changed as fish shifted from aquatic to terrestrial lifestyles[15,16]. *Panderichthys rhombolepis*[1-3], *Tiktaalik roseae*[4-8] and *Elpistostege watsoni*[9] hold a special place in these analyses, showing a combination of plesiomorphic and apomorphic features that give insight into a sequence of anatomical changes in the origin of limbed taxa (*i.e.*, those in possession of digited appendages and lacking dermal rays). Currently missing, however, is an understanding of the morphological, functional, and ontogenetic diversity of the finned tetrapodomorphs most closely related to limbed forms. This is unfortunate, as isolated or fragmental specimens have controversially hinted at a wider range of diversity than is observed in more complete material[10-14].

Here we describe a new finned tetrapodomorph that is closely related to *T. roseae* and *E. watsoni*. The new form exhibits an unexpected combination of characters, one that suggests a broad range in disparity among the closest finned relatives of limbed forms. The specimen was collected 1.5 km east of the site that yielded *T. roseae,* but from a slightly lower horizon within the Fram Formation of southern Ellesmere Island, Nunavut Territory, Canada. We describe this novel taxon and present a phylogenetic analysis to reveal its implications for understanding the evolution of the nearest relatives of limbed tetrapodomorphs. Comparison of the new taxon to other Frasnian-age forms allows a reinterpretation of isolated elements of previously uncertain affinity, thus, indicating a more widespread and diverse assemblage of tetrapod relatives than previously recognized.

Geological framework

Embry and Klovan[17] described the type section of the Fram Formation from a drainage feeding the eastern arm of Bird Fiord on southern Ellesmere Island. They indicate an Early to Middle Frasnian age for the Fram Formation based on palynological spot samples, which were collected from near the base, the middle and top of the formation[17]. The Nunavut Paleontological Expeditions collected vertebrate remains from 2000 to 2008 at 16 sites from the Fram Formation within the type section. The holotype of *T. roseae* (NUFV 108), as well as all other *T. roseae* specimens, were collected from site NV2K17, which occurs within silty overbank floodplain deposits[18] at 533 m above the base of the measured type section of Embry and Klovan[17]. The specimen discussed here (NUFV 137) was collected at site NV0401 (N77°10.235’ W86°11.279’) from lower in the same section and 1.5 km from NV2K17 (Fig. 1 a,b; Extended Data Fig. 1). Site NV0401 is about 453 m above the base of the type section and occurs within a medium-grained sandstone. The surface-collected NUFV 137 is the only specimen found at the site. NUFV 137 is older than *T. roseae* and was collected from a different facies within the floodplain deposits of the Fram Formation.

Systematic Paleontology

Sarcopterygii Romer, 1955

Tetrapodamorpha Ahlberg, 1991

Elpistostegalia Camp and Allison, 1961

Qikiqtania wakei gen. et sp. nov.

Locality. Canada, Nunavut Territory, southern Ellesmere Island, near the eastern arm of Bird Fiord, Nunavut Paleontological Expedition site NV0401, N77°10.235' W86°11.279'.

Geological Setting. Fram Formation (Upper Devonian, early Frasnian Stage).

Etymology. *Qikiqtania (*pronounced "*kick-kiq-tani-ahh*"*)* is derived from Inuktitut word Qikiqtaaluk/Qikiqtani, the traditional name for the region where the fossil site occurs. The species designation is in memory of David Wake, an eminent evolutionary biologist and transformative mentor, late of the University of California at Berkeley.

Holotype. Nunavut Fossil Vertebrate Collection (NUFV) 137.

Material. The description is based on a specimen from the NV0401 site that preserves the symphysis of the lower jaw, partial left upper jaw and palate in articulation, gulars, ceratohyals, an articulated left pectoral fin, and articulated scales from the dorsal midline, flank, and lateral line series (Fig. 1 c, Extended Data Fig. 2). The jaw material was physically prepared at the Academy of Natural Sciences of Drexel University. Computed tomography (CT) scans were collected at The University of Chicago's PaleoCT scanning facility (Table S1). Specimens will be housed at the Canadian Museum of Nature, Ottawa, Ontario, until such time as research and collections facilities are available within the Nunavut Territory.

Diagnosis. Elpistostegalian tetrapodomorph characterized by the following unique combination of characters: dorsoventral asymmetry in pectoral fin lepidotrichia (also present in *T. roseae*) and possession of a boomerang-shaped humerus lacking ventral ridge and associated foramina and ectepicondyle (distinct from *P. rhombolepis*, *E. watsoni*, *T. roseae* and more crownward tetrapods).

Description

Upper jaw and palate. Rostral elements of the upper jaws and palate, including portions of the ectopterygoid, dermopalatine, vomer, premaxilla, and maxilla are preserved (Fig. 2 a,b; Extended Data Fig. 2; Video S2). These elements are primarily from the left side and preserved in articulation with the lower jaws. The vomer is broad, fanged, and forms the posterior wall of the palatal fossa with a row of smaller teeth. Fangs and a row of smaller teeth are also present on the dermopalatine and ectopterygoid. An expanded mesial surface of the dermopalatine lacks teeth and overlaps slightly with the vomer, similar to *T. roseae*[8], forming the mesial and posterior margin of the choana. The anterolateral wall of the choana is formed by a simple, smooth articulation of the premaxilla and maxilla. Maxillary teeth are smaller than the premaxillary teeth. Within their respective tooth rows, maxillary and premaxillary teeth are uniform in size.

Lower jaw. The lower jaws of *Q. wakei* are preserved in articulation anterior to the adductor chamber, including the dentary, infradentaries, coronoids, and prearticular (Fig. 2). The symphysis is relatively smooth, not interdigitating. Large fangs with plicidentine infolding are present on the dentary, anterior coronoid, and middle coronoid. Rows of smaller dentition are also present on the coronoids and dentary, including evidence of an auxiliary lateral tooth row on the dentary. The prearticular has a broad shagreen field of denticles that is raised adjacent to coronoids, and the denticles possess a distinct dorsoventral gradient in size. The adsymphyseal is missing, but small teeth embedded in the matrix of the precoronoid fossa suggest it was present in life.

Infradentaries are identifiable by the presence of the mandibular canal and postsplenial pit line. The mandibular canal is an open groove along most of its length, but in areas of the most intact preservation it takes the form of discrete pits the bone surface. The splenial has a larger post-symphyseal flange than in *T. roseae* but has a similar articulation with the prearticular[4]. Boundaries between the infradentaries are obscured by overlying dermal sculpting and are difficult to distinguish in CT cross-section.

The meckelian canal contains only partially ossified meckelian bone along its length, but evidence of meckelian ossification extends from the symphysis to the posterior coronoids. The canal is exposed lingually ventral to the prearticular, and, in areas of intact ossification, meckelian fenestra are bordered dorsally by meckelian bone and ventrally by infradentaries.

Gular plates and ceratohyal. Fragments of a principal and median gular plate are preserved, along with a series of submandibulo-branchiostegal plates (Fig. 2 a,b). A grooved ceratohyal lies immediately adjacent to the left lower jaw.

Pectoral fin. The left pectoral fin includes the humerus, ulna, radius, intermedium, third mesomere, third radial, fin web and associated scales (Fig. 3 a,b; Video S3). The fin is embedded in matrix with the proximal articular surface of the humerus and the posterior distal fringe of the fin web exposed at the edges of the block (Extended Data Fig. 3 a). Three endoskeletal elements contact the humerus. Two have robust proximal articular surfaces and are identified as the radius and ulna. The third, which lies between and slightly dorsal to them, is identified as the intermedium proximally displaced during preservation, although its shape is difficult to assess due to its position relative to other elements (Fig. 3 c,d, see Supplementary Discussion).

The fin is characterized by ventralward curvature of the radius and asymmetry in the lepidotrichia, where dorsal hemitrichia have a greater cross sectional area than ventral hemitrichia, as in *T. roseae* (Fig. 3 e; Extended Data Fig. 3 c,d)[7]. Approximately thirty lepidotrichia are preserved. Similar to other finned tetrapodomorphs, rays are more robust anteriorly and more gracile posteriorly, and rays are more terminally positioned on the posterior side[7].

The humerus is boomerang shaped and lacks numerous characteristic elpistostegalian features, notably a humeral ridge and associated foramina, ectepicondylar process, prominent entepicondyle, and distinct articular surfaces for the ulna and radius (Fig. 3 f-k). The ulna lacks a post-axial process and distally would have articulated with the intermedium and ulnare. The fin is gracile as compared to other elpistostegalians. The anteroposterior width of the humerus is narrower than the humeri of *T. roseae*[5] and *E. watsoni*[9] and more similar to *P. rhombolepis*[3]. The shallow dorsoventral depth of the fin might reflect compression; however, articular surfaces of the ulna and radius are similar in their geometry to three-dimensionally preserved specimens of *T. roseae,* suggesting that morphology was narrow in life (see Supplementary Discussion).

Scalation. Scales are preserved from the trunk, including dorsal midline and flank, the pectoral fin, and the lateral line series (Extended Data Fig. 4). Scalation is broadly similar to other finned elpistostegalians[7,9,22]. Scales are rhomboid in shape with the free surface sculpted and a smooth internal surface that often bears a ventral keel (Extended Data Fig. 4 a-c). On the trunk, scale rows extend posterolaterally from the dorsal midline, with individual scales partially covering the scale that follows in the row and also the scale of an adjacent posterior row (Extended Data Fig. 1 d,e). Pectoral fin scales are smaller than those of the flank and show variation in their morphology (Extended Data Fig. 4 f-m). Lateral line scales are preserved from the left flank and show a completely enclosed tube with anterior suprascalar and posterior infrascalar pores enlarged relative to the diameter of the canal, and a small pore midway along the length of the scale connecting the canal to the external environment (Extended Data Fig. 4 n-r).

Phylogenetic relationships

The phylogenetic position of *Q. wakei* was analyzed by maximum parsimony (MP) and undated Bayesian approaches, which were applied to a matrix of 13 taxa and 125 characters primarily assembled from previous publications[9,23,24]. Both methods robustly recover *Q. wakei* as crownward to *P. rhombolepis* and, thus, as an elpistostegalian closely related to limbed tetrapods (Fig. 4). The analyses differ in their relative placement of *Q. wakei*, *T. roseae*, *E. watsoni*; a strict consensus tree of the 28 shortest trees recovered from MP analyses shows an unresolved polytomy, whereas Bayesian analysis finds weak support for a sister relationship between *Q. wakei* and *T. roseae* with *E. watsoni* positioned more crownward. This is similar to other recent phylogenetic analyses of stem tetrapods, which have robustly recovered *Tiktaalik* and

Elpistostege as outgroups to digited forms, although support for their relative positions is not strong[9,23,25].

Discussion

Qikiqtania wakei reveals a combination of characters unique among stem tetrapods. The pectoral fin, lacking a postaxial process on the ulnare and exhibiting accentuated hemitrichial asymmetry, is clearly elpistostegalian[5,7]. Yet, the morphology of the humerus is unlike others described. With the absence of a ventral ridge or ectepicondylar process and in possession of a general boomerang shape, it is more similar to the humerus previously attributed to the tetrapod, *Elginerpeton pancheni*[10], than to any other Devonian taxon (Fig. 5). That specimen, GSM 104536, from Scat Craig in Scotland, is an isolated bone from a coeval deposit in Laurentia that generated debate as to whether it was from a tetrapod or whether it was even a humerus at all[10-14]. The similarity to *Q. wakei* suggests that GSM 104536 is indeed a humerus but belongs to a finned elpistostegalian, not a limbed tetrapod.

The morphology of the *Q. wakei* humerus is distinctive among stem tetrapods. Indeed, the lack of muscular processes on the humerus for flexors and extensors at the shoulder and elbow, the terminal position of the facets for the radius and ulna, and the relatively large surface area of the fin web suggest that the fin of *Q. wakei* is less suited for walking, trunk lifting and station holding in water than it is for a range of swimming behaviors[13]. With its gracile form and lacking many of the known major osteological correlates of muscular attachment[26], the pectoral fin of *Q. wakei* represents a strategy of controlling hydrodynamic forces not seen in other stem tetrapods. As these features are not seen in tristichopterids, osteolepids or rhizodontids, they likely arose as apomorphies within elpistostegalians.

The holotype of *Q. wakei* is estimated to be 75 cm standard length (calculated from the proportions of *E. watsoni* specimen MHNM 06-2067[9] scaled to the length of the lower jaw), making it smaller than other described elpistostegalians. The ontogenies of *Eusthenopteron foordi* and *T. roseae* provide evidence that, despite its relatively small size, the unique humeral morphology of *Q. wakei* reflects phylogenetic signal and not developmental stage. *E.*

foordi individuals are described spanning more than 40-fold variation in size[27], and across a broad range of sizes uniformly retain a ventral ridge, entepicondylar process, and orientations of facets for articulation with the radius and ulna[28,29]. *T. roseae*, which is known from humeri ranging two-fold in size, show a similar pattern, preserving these features across this size range, although overall proportions might vary[5,7]. Thus, major ontogenetic shifts in limb skeletal anatomy of *Ichthyostega* and *Acanthostega*, implied to correspond to aquatic subadults transitioning to more terrestrial adult lifestyles utilizing appendage-based substrate support, are derived for limbed forms[30]. Finned tetrapodomorphs**,** by contrast, are predicted to show more minor changes in the proportions of endoskeletal, and potentially dermal, components of their paired fins[7].

With two elpistostegalian genera now known from nearby localities in Canadian Arctic and others from Quebec[9], Latvia[31,32] and potentially Russia[33], Australia[34] and Scotland[10], the group likely has a wide distribution by the Frasnian Stage of the Late Devonian. This broad biogeographic range, coupled with the morphological disparity revealed by *Q. wakei*, hints at a wider diversity of elpistostegalians than currently known, with the closest relatives of tetrapods adapting in novel ways to benthic, littoral, and open water habitats by the Late Devonian[25,35].

References

1 Boisvert, C. A. The pelvic fin and girdle of *Panderichthys* and the origin of tetrapod locomotion. *Nature* **438**, 1145-1147, doi:10.1038/nature04119 (2005).

2 Boisvert, C. A., Mark-Kurik, E. & Ahlberg, P. E. The pectoral fin of *Panderichthys* and the origin of digits. *Nature* **456**, 636-638 (2008).

3 Boisvert, C. A. The humerus of *Panderichthys* in three dimensions and its significance in the context of the fish–tetrapod transition. *Acta Zoologica* **90**, 297-305, doi:https://doi.org/10.1111/j.1463-6395.2008.00389.x (2009).

4 Daeschler, E. B., Shubin, N. H. & Jenkins, F. A. A Devonian tetrapod-like fish and the evolution of the tetrapod body plan. *Nature* **440**, 757-763, doi:http://www.nature.com/nature/journal/v440/n7085/suppinfo/nature04639_S1.html (2006).

5 Shubin, N. H., Daeschler, E. B. & Jenkins, F. A. The pectoral fin of *Tiktaalik roseae* and the origin of the tetrapod limb. *Nature* **440**, 764-771, doi:http://www.nature.com/nature/journal/v440/n7085/suppinfo/nature04637_S1.html (2006).

6 Shubin, N. H., Daeschler, E. B. & Jenkins, F. A. Pelvic girdle and fin of *Tiktaalik roseae*. *Proceedings of the National Academy of Sciences* **111**, 893-899, doi:10.1073/pnas.1322559111 (2014).

7 Stewart, T. A. *et al.* Fin ray patterns at the fin-to-limb transition. *Proceedings of the National Academy of Sciences* **117**, 1612-1620, doi:10.1073/pnas.1915983117 (2020).

8 Lemberg, J. B., Daeschler, E. B. & Shubin, N. H. The feeding system of *Tiktaalik roseae*: an intermediate between suction feeding and biting. *Proceedings of the National Academy of Sciences* **118**, e2016421118, doi:10.1073/pnas.2016421118 (2021).

9 Cloutier, R. *et al. Elpistostege* and the origin of the vertebrate hand. *Nature* **579**, 549-554, doi:10.1038/s41586-020-2100-8 (2020).

10 Ahlberg, P. E. Postcranial stem tetrapod remains from the Devonian of Scat Craig, Morayshire, Scotland. *Zoological Journal of the Linnean Society* **122**, 99-141, doi:https://doi.org/10.1006/zjls.1997.0115 (1998).

11 Ahlberg, P. Comment on "The early evolution of the tetrapod humerus". *Science* **305** (2004).

12 Coates, M., Shubin, N. & Daeschler, E. Response to comment on "The early evolution of the tetrapod humerus". *Science* **305**, 1715 (2004).

13 Shubin, N. H., Daeschler, E. B. & Coates, M. I. The Early Evolution of the Tetrapod Humerus. *Science* **304**, 90-93, doi:10.1126/science.1094295 (2004).

14 Ahlberg, P. E. Humeral homology and the origin of the tetrapod elbow: a reinterpretation of the enigmatic specimens ANSP 21350 and GSM 104536. *Special Papers in Paleontology* **86**, 17-29 (2011).

15 Clack, J. A. *Gaining Ground: The origin and evolution of tetrapods*. 2 edn, 544 (Indiana University Press, 2012).

16 Coates, M., Ruta, M. & Friedman, M. Ever Since Owen: Changing Perspectives on the Early Evolution of Tetrapods *Annu. Rev. Ecol. Evol. Syst.* **39**, 571-592 (2008).

17 Embry, A. & Klovan, J. E. The Middle–Upper Devonian clastic wedge of the Franklinian Geosyncline. *Bulletin of Canadian Petroleum Geology* **24**, 485–639 (1976).

18 Miller, J. H., Shubin, N., Daeschler, E. & Downs, J. Stratigraphic context of *Tiktaalik roseae* (Late Devonian): Paleoenvironment of the fish-tetrapod transition. *Geological Society of America Annual Meeting - Abstracts with Programs* **39**, 417 (2007).

19 Romer, A. S. Herpetichthyes, Amphibioidei, Choanichthyes, or Sarcopterygii? *Nature* **176**, 126 (1955).

20 Ahlberg, P. E. A re-examination of sarcopterygian interrelationships, with special reference to the Porolepiformes. *Zool. J. Linn. Soc.* **103**, 241–-287 (1991).

21 Camp, C. L. & Alison, H. J. Bibliography of fossil vertebrates 1949–-1953. *Geol. Soc. Am. Mem.* **84**, 1–-53 (1961).

22 Witzmann, F. Morphological and histological changes of dermal scales during the fish-to-tetrapod transition. *Acta Zoologica* **92**, 281-302, doi:https://doi.org/10.1111/j.1463-6395.2010.00460.x (2011).

23 Ahlberg, P. E. & Clack, J. A. The smallest known Devonian tetrapod shows unexpectedly derived features. *Royal Society Open Science* **7**, 192117, doi:doi:10.1098/rsos.192117 (2020).

24 Swartz, B. A Marine Stem-Tetrapod from the Devonian of Western North America. *PLOS ONE* **7**, e33683, doi:10.1371/journal.pone.0033683 (2012).

25 Simões, T. R. & Pierce, S. E. Sustained high rates of morphological evolution during the rise of tetrapods. *Nature Ecology & Evolution*, doi:10.1038/s41559-021-01532-x (2021).

26 Molnar, J. L., Diogo, R., Hutchinson, J. R. & Pierce, S. E. Reconstructing pectoral appendicular muscle anatomy in fossil fish and tetrapods over the fins-to-limbs transition. *Biological Reviews* **93**, 1077-1107, doi:10.1111/brv.12386 (2018).

27 Cloutier, R., Béchard, I., Charest, F. & Matton, O. La contribution des poissons fossiles du parc national de Miguasha à la biologie évolutive du développement. *Le Naturaliste canadien* **133**, 84-95 (2009).

28 Andrews, S. M. & Westoll, T. S. IX.—The Postcranial Skeleton of *Eusthenopteron foordi* Whiteaves. *Transactions of the Royal Society of Edinburgh* **68**, 207-329, doi:10.1017/S008045680001471X (1970).

29 Schultze, H.-P. Juvenile specimens of *Eusthenopteron foordi* Whiteaves, 1881 (osteolepiform rhipidistian, Pisces) from the Late Devonian of Miguasha, Quebec, Canada. *Journal of Vertebrate Paleontology* **4**, 1-16, doi:10.1080/02724634.1984.10011982 (1984).

30 Callier, V., Clack, J. A. & Ahlberg, P. E. Contrasting Developmental Trajectories in the Earliest Known Tetrapod Forelimbs. *Science* **324**, 364-367, doi:10.1126/science.1167542 (2009).

31 Gross, W. Über den Unterkiefer einiger devonischer Crossopterygier. *Abhandlungen der Preußischen Akademie der Wissenschaften, Mathematische und Naturwissenschaftliche Klasse* **7**, 3-51 (1941).

32 Ahlberg, P., Lukševičs, E. & Mark-Kurik, E. A near-tetrapod from the Baltic Middle Devonian. *Palaeontology* **43**, 533-548, doi:https://doi.org/10.1111/j.0031-0239.2000.00138.x (2000).

33 Vorobyeva, E. I. Rizodontnyye kisteperyye ryby Glavnogo devonskogo polya SSSR *Trudy Paleontologicheskogo Institua* **104**, 1-141 (1962).

34 Long, J. A. & Holland, T. A possible elpistostegalid from the Devonian of Gondwana. *Proceedings of the Royal Society of Victoria* **120**, 182–192 (2008).

35 Ruta, M., Krieger, J., Angielczyk, K. D. & Wills, M. A. The evolution of the tetrapod humerus: morphometrics, disparity, and evolutionary rates. *Earth and Environmental Science Transactions of the Royal Society of Edinburgh* **109**, 351-369, doi:10.1017/S1755691018000749 (2018).

36 Clement, A. M. *et al.* A fresh look at *Cladarosymblema narrienense*, a tetrapodomorph fish (Sarcopterygii: Megalichthyidae) from the Carboniferous of Australia, illuminated via X-ray tomography. *PeerJ* **9**, e12597, doi:10.7717/peerj.12597 (2021).

37 Coates, M. I. The Devonian tetrapod *Acanthostega gunnari* Jarvik: postcranial anatomy, basal tetrapod interrelationships and patterns of skeletal evolution. *Transactions of the Royal Society of Edinburgh: Earth Sciences* **87**, 363-421, doi:10.1017/S0263593300006787 (1996).

38 Swofford, D. L. PAUP* Phylogenetic Analysis Using Parsimony (*and Other Methods), Version 4. (Sinauer Associates, Sunderland, Massachusetts, 2003).

39 Bremer, K. Branch Support and Tree Stability. *Cladistics* **10**, 295-304, doi:https://doi.org/10.1111/j.1096-0031.1994.tb00179.x (1994).

40 AutoDecay (Bergius Foundation, Royal Swedish Academy of Sciences, Stockholm, 2001).

41 Ronquist, F. & Huelsenbeck, J. P. MRBAYES 3: Bayesian phylogenetic inference under mixed models. *Bioinformatics* **19**, 1572-1574 (2003).

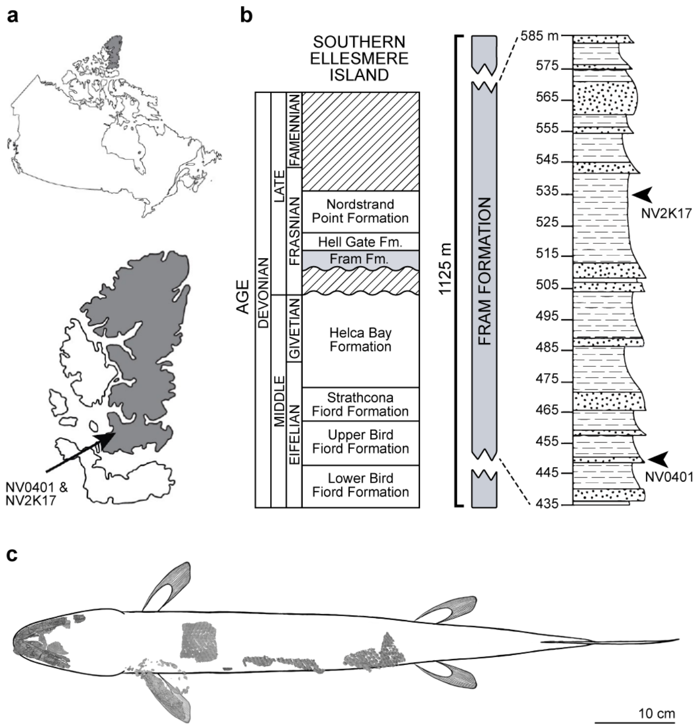

Fig. 1. Locality and holotype of *Qikiqtania wakei* gen. et sp. nov. (a) Specimen NUFV 137 was discovered on southern Ellesmere Island, Nunavut Territory, Canada. (b) The site, NV0401, lies 80 m below NV2K17, the site where *T. roseae* was discovered. (c) Materials were µCT scanned and are shown here in dorsal aspect. General body shape based on specimen MHNM 06-2067 of *E. watsoni*[9].

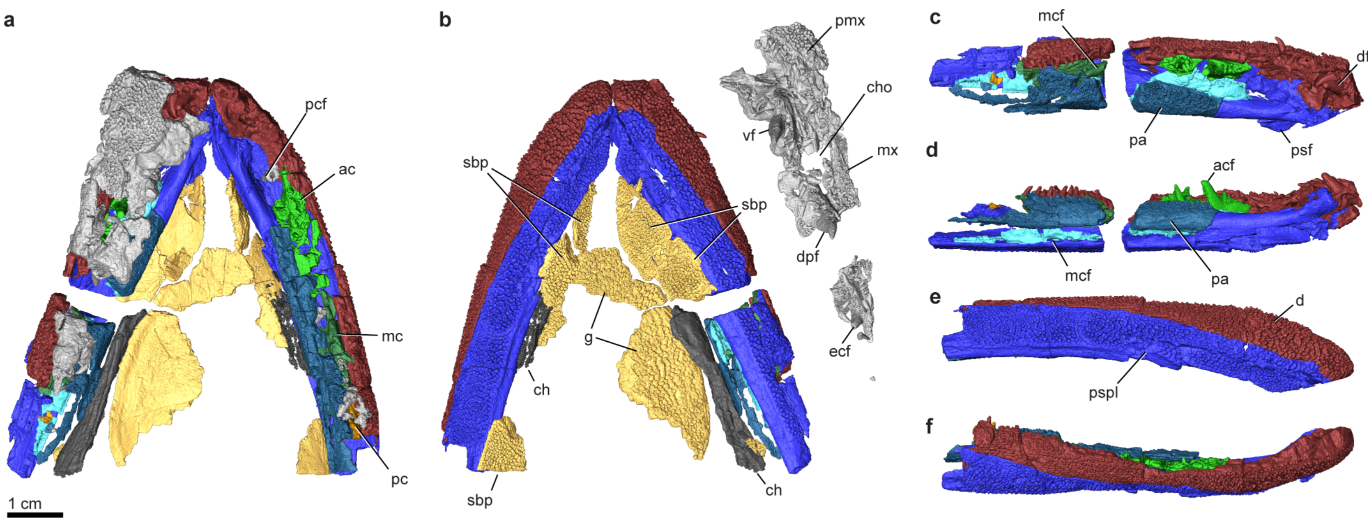

Fig. 2. The feeding apparatus of *Qikiqtania wakei*. Volume renderings of µCT scans of the lower jaw and additional fragments reconstructed in their natural positions. (a) Dorsal view of the lower jaws, ceratohyal, gular plates, premaxilla, and palate. (b) Ventral view with premaxillary and palatal elements displaced so ventral surfaces are visible. (c) Left lower jaw, dorsal. (d) Left lower jaw, medial. (e) Right lower jaw, ventral. (f) Right lower jaw, lateral. Abbreviations: ac, anterior coronoid; acf, anterior coronoid fang; ch, ceratohyal; cho, choana; d, dentary; df, dentary fang; dpf, dermopalatine fang; ecf, ectopterygoid fang; g, gulars; mc, meckel's cartilage; mcf, meckelian canal foramen; mx, maxilla; pa, prearticular; pc, posterior coronoid; pcf, precoronoid fossa; pmx, premaxilla; pspl, postsplenial; sbp, submandibulo-branchiostegal plate; psf, post-symphyseal flange; vf, vomerine fang.

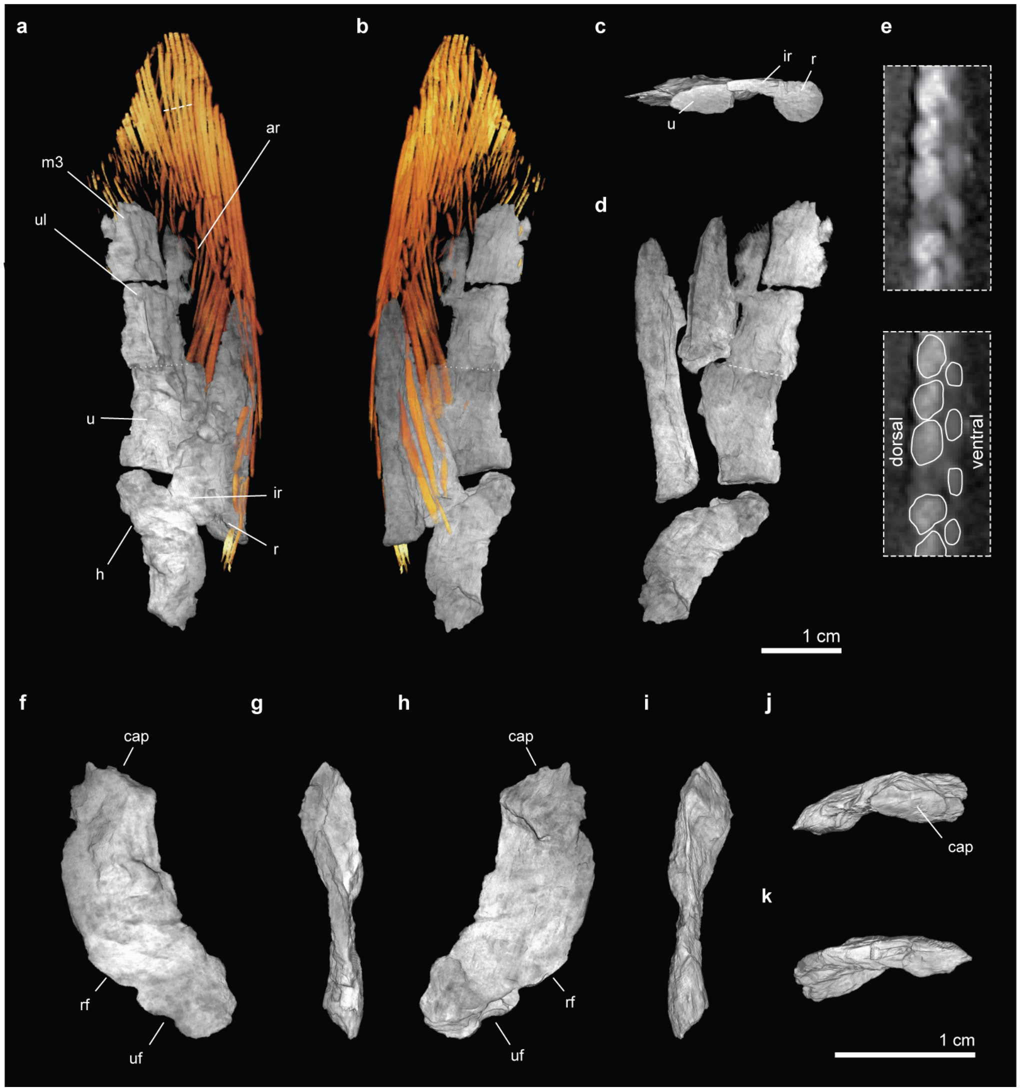

Fig. 3. Left pectoral fin of *Qikiqtania wakei*. Volume renderings of µCT scans of the fin with scales removed. (a) Dorsal and (b) ventral views of the fin with endoskeleton in grey and dermal rays in orange. Dotted lines indicate the boundary between ulna and ulnare. The dashed line indicates position of cross section in panel e, which is oriented orthogonal to the plane of the fin web. (c) Endoskeleton viewed from the proximal side with humerus removed. (d) Reconstruction of endoskeletal elements with estimated boundary between the radius and intermedium. (e) Cross sections of the fin rays, showing asymmetry in the size of dorsal and ventral hemitrichia. Humerus in (f) dorsal, (g) pre-axial (anterior), (h) ventral, (i) post-axial (posterior), (j) proximal, and (k) distal perspectives. Proximal is up in panels f-i. Dorsal is up in panels j and k.

Abbreviations: ar, anterior radial; cap, caput humeri; h, humerus; ir, intermedium; r, radius; rf, radial facet; m3, third mesomere, u, ulna; ul, ulnare; uf, ulnar facet.

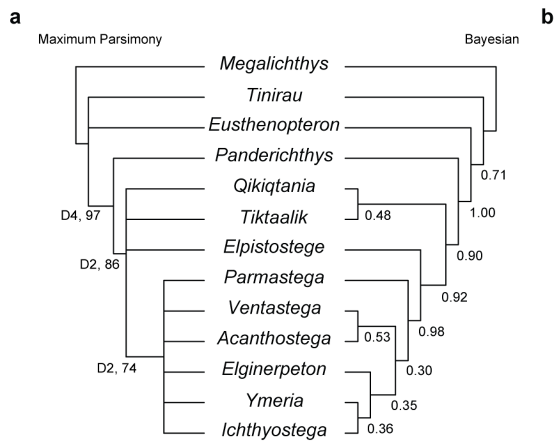

Fig. 4. Phylogenetic analysis. (a) Strict consensus tree from the maximum parsimony analysis with Bremer decay (D) and bootstrap support values. (b) Majority rule tree from undated Bayesian analysis with posterior probabilities. Both analyses recover a basal polytomy; *Megalichthys* is shown as the outgroup, consistent with other studies[9,23,25,36].

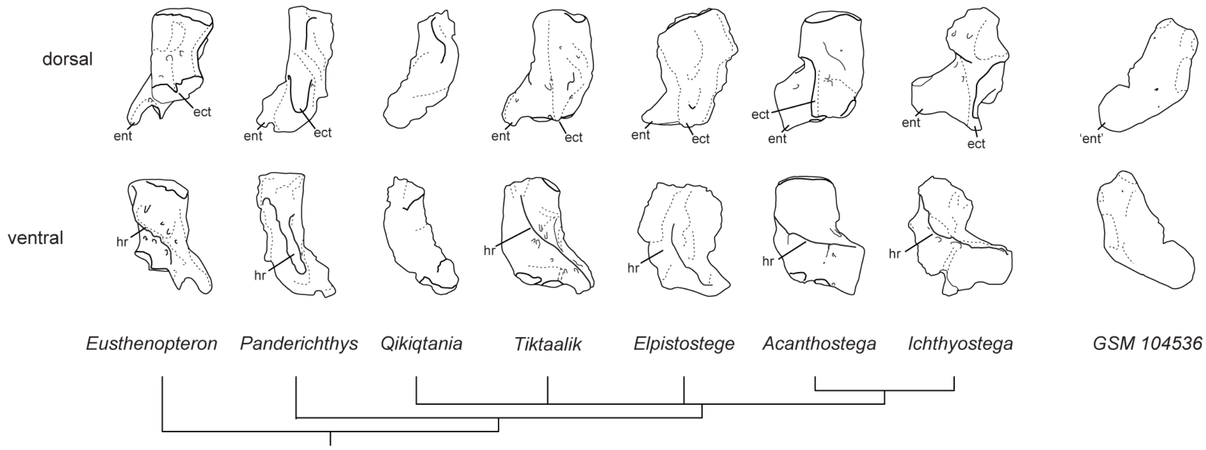

Fig. 5. Humeri at the fin-to-limb transition. For consistency of orientation between species, several specimens have been reflected, so that each is represented as being from the right side. Illustrations are based upon previously published descriptions: *Eusthenopteron*[28], *Panderichthys*[2,3], *Tiktaalik*[5], *Elpistostege*[9], *Acanthostega*[37], *Ichthyostega*[30], GSM 104536[10,14]. Abbreviations: ect, ectepicondyle; ent, entepicondyle; hr, humeral, or ventral, ridge.

Methods

Computed tomography scanning

CT scans were collected at The University of Chicago's PaleoCT scanning facility using a GE Phoenix v|tome|x 240 kv/180 kv scanner (http://luo-lab.uchicago.edu/paleoCT.html). Scan parameters are reported in Table S1. CT data were reconstructed with Phoenix Datos|x 2 (v2.3.3), imported to VGStudio Max (v2.2) for cropping and exportation as a 16-bit tiff stack. Tiff stacks were segmented and visualized in Amira v20.2 (FEI Software). For some scans, to accommodate for computational challenges that arise from large file sizes, data were converted to 8-bit files for segmentation; in such cases, after segmentation the renderings were generated from the original 16-bit files. Animations were generated by exportation tiff stacks from Amira and then edited with Adobe Premiere (v13.12). High-resolution versions of images from all figures are provided in Data S1.

Phylogenetic analyses

We investigated the phylogenetic position of *Q. wakei* using a phylogenetic data set of 13 taxa and 125 characters. All characters were treated as equally informative, and we assumed unordered evolution among states.

Maximum parsimony analyses were performed using PAUP* (v4.0a168)[38]. The branch and bound method for searching tree space was used with the command "bandb" with no topological constraints. A total of 28 most-parsimonious trees were recovered (tree length = 151). The trees are summarized as a strict consensus tree (Fig. 4) and as an Adams consensus tree (Extended Data Fig. 5 a). Clade support was estimated using two approaches: Bremer decay values[39], calculated with AutoDecay (v5.06)[40], and non-parametric bootstrapping, calculated in PAUP* with 500 replicates (Fig. 4, Extended Data Fig. 5 b). Apomorphies of nodes in the strict consensus tree were identified using the function 'apolist' in PAUP*, which returns characters optimized under both accelerated transformation (ACCTRAN) and delayed transformation (DELTRAN) conditions (Extended Data Fig. 5 c).

Undated Bayesian analyses were performed using MrBayes (v3.2.7a)[41]. Analyses were run for five million generations with 4 runs of 4 chains sampling every 5000 generations and a burn-in of 20%. *Megalichthys* was designated as an outgroup, consistent with other studies[9,23,25,36]. Convergence was assessed with diagnostics reported by MrBayes (avg. SD of split frequencies < 0.02, potential scale reduction factors = 1, effective sample sizes > 200). Results are summarized by a majority-rule consensus tree of post-burn-in trees (Fig. 4).

For both maximum parsimony and Bayesian analyses, executable files, log files, and individual trees that contribute to the summary trees are included as supplementary files (Data S2, S3).

Data and code availability

All data and code used in the paper are freely available. All computed tomography data sets and STL files of major elements are available for download from MorphoSource (https://www.morphosource.org/projects/000375542). Executable files for PAUP* and MrBayes are available in the supplementary materials. Code for the calculation of Bremer decay values and for visualization of phylogenies are available at https://github.com/ThomasAStewart/Qikiqtania

Acknowledgments: Fieldwork was made possible by the Polar Continental Shelf Project of Natural Resources, Canada; Department of Heritage and Culture, Nunavut; the hamlets of Resolute Bay and Grise Fiord of Nunavut; the Iviq Hunters and Trappers of Grise Fiord. Sylvie Leblanc (Department of Heritage and Culture, Nunavut) assisted with permits and in the exploration of a scientific name for the new fossil. We thank Fred Mullison for fossil preparation and Mark Webster for assistance trimming the fin block prior to scanning. This work was supported by: The Brinson Foundation; Anonymous donor to the Academy of Natural Sciences of Drexel University; The Biological Sciences Division of The University of Chicago; the National Science Foundation under Grants EAR 0207721 (to EBD), EAR 0544093 (to EBD), EAR 0208377 (to NHS), and EAR 0544565 (to NHS).

Author contributions: NS and EBD led fieldwork; NS found specimen; JL, TS, and AD performed imaging analyses; TS, JL, EBD, and NS undertook character analyses; TS did phylogenetic analyses; TS, JL, EBD and NS wrote paper.

Competing interests: Authors declare that they have no competing interests.

Supplementary Information is available for this paper.

Correspondence and requests for materials should be addressed to Dr. Neil Shubin (nshubin@uchicago.edu).

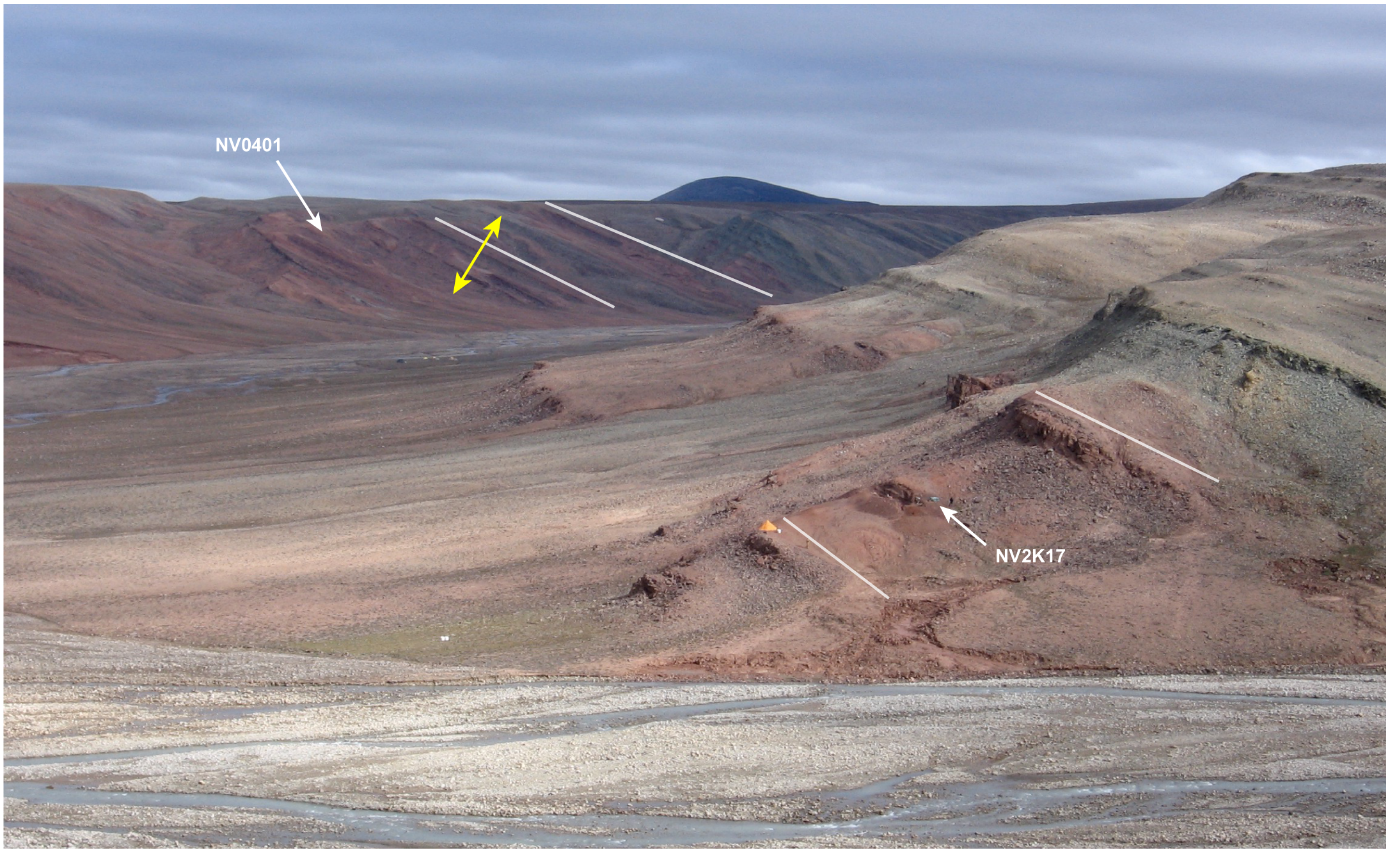

Extended Data Figure 1 | Photograph of the locality NV0401.

Photograph showing the localities NV0401, where NUFV 137 was collected, and NV2K17, where *T. roseae* was collected. White arrows indicate sites of collection. Yellow arrows highlight approximate stratigraphic separation between the two horizons. White lines trace two additional horizons across the valley. A yellow tent, approximately 2.5 m across, is in the midground.

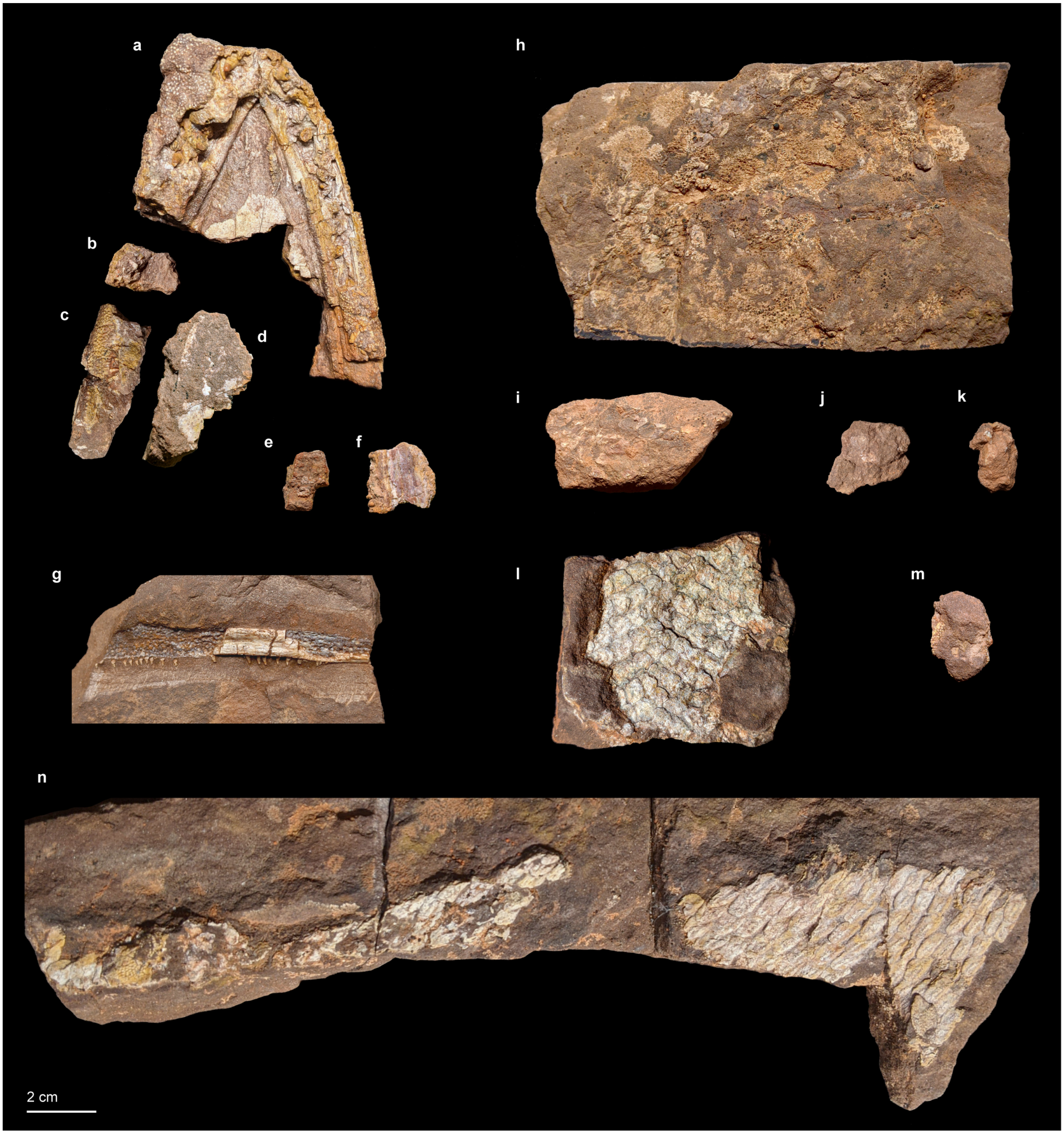

Extended Data Figure 2 | Photographs of NUFV 137.

(a-f) Elements associated with the feeding apparatus. Elements in a-d are shown in Fig. 2 and Video S2. Element e is identified as parts of the palate and lower jaw due to the presence of multiple rows of both dorsally and ventrally facing teeth. The ventrally facing teeth are determined to be palatal in nature due to the expanded medial shagreen of denticles (likely part of the entopterygoid) that are bordered laterally by two uniform rows of larger teeth (likely the ectopterygoid and maxilla). This piece could not be definitively positioned relative to the other jaw elements due to absence of the corresponding broken tooth bases on the main lower jaw block. Element f is identified as part of a lower jaw on the basis of its curvature and dentition. (g) Maxilla. (h) Left pectoral fin, which is embedded in matrix, with exposed associated scales. (i) Fragment containing scales and lepidotrichia from a paired fin. (j, k) Fragments with undiagnosed vascularized endoskeletal elements. (l) Scale field from the dorsal midline, anterior is up. (m) Fragment containing scales from the lateral line series and flank. (n) Trunk scale field, anterior is left.

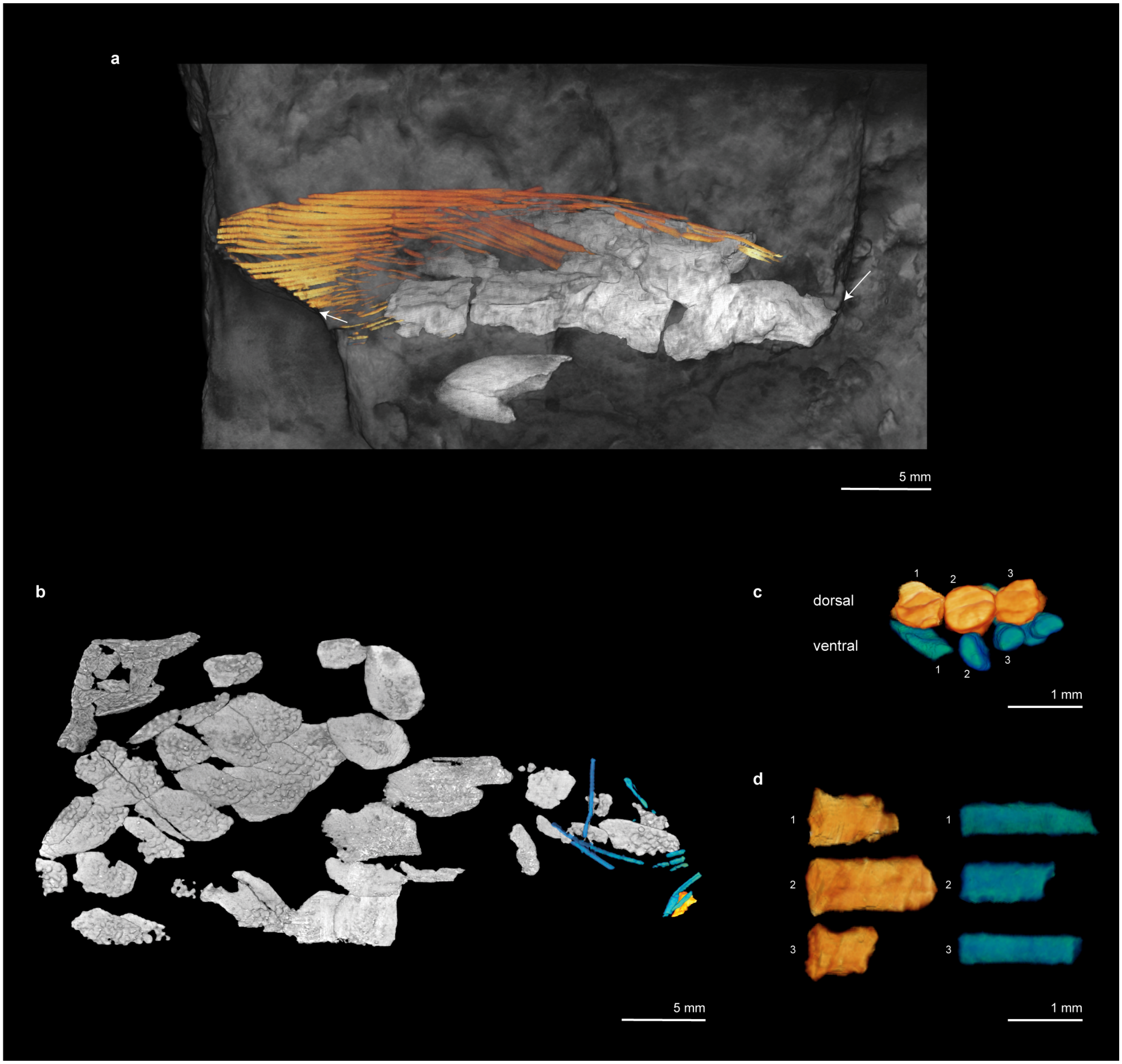

Extended Data Figure 3 | Additional fin-associated materials.

(a) A thin, slightly convex bladelike element that might be part of the pectoral girdle is adjacent to the pectoral fin. Breaks in the block have exposed the proximal articular surface of the humerus and the posterodistal portion of the fin web. (b) An element, shown in Extended Data Fig. 2 i, contains scales and additional lepidotrichia from a paired fin. (c) Fin rays, seen in the lower right corner of panel b, in their preserved position showing asymmetry between the dorsal and ventral hemitrichia. (d) Three pairs of hemitrichia from panel c repositioned and shown in dorsal perspective. Dorsal hemitrichia are orange, and ventral hemitrichia are blue.

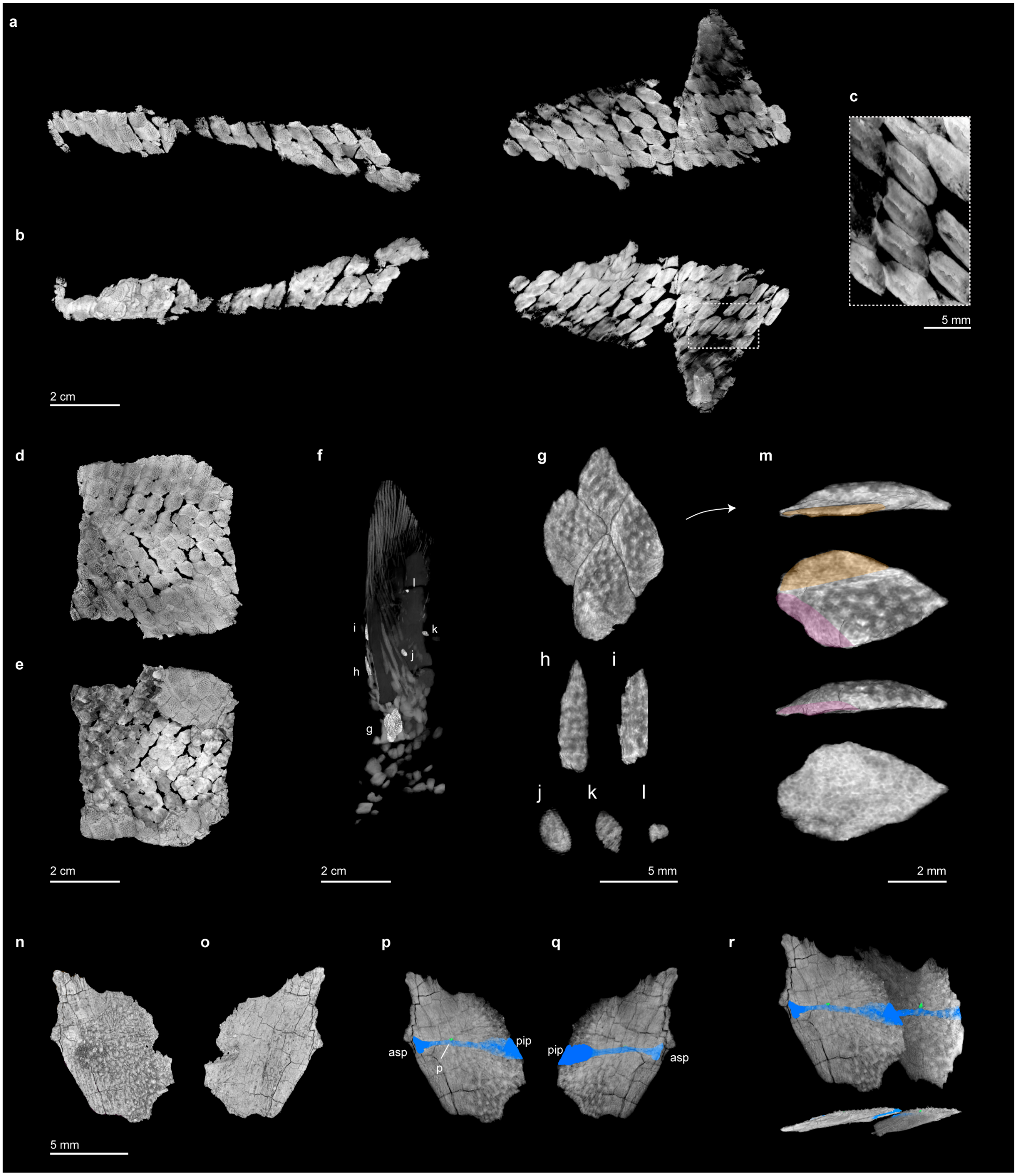

Extended Data Figure 4 | NUFV 137 scales.

Internal (a) and external (b) views of scale field from left flank. (c) Scales outlined in panel b showing median ridge on internal surface. Internal (d) and external (e) views of scale field from dorsal midline. (f) Left pectoral fin in ventral aspect showing the position of individual scales figured in panels g-l. (g) Scales that covered the humerus ventrally. (h, i) Elongate scales from leading edge. (j-l) Small scales from the ventral surface of the fin. (m) One scale in pre-axial (anterior), external, post-axial (posterior) and internal views showing dermal sculpting and lack of ventral keel. (n, o) Left lateral line scale in external and internal views. (p, q) Scale with reduced opacity and the canal shown in blue. Midway along the length of the scale, a pore connects fluid in the canal and the external environment. (r) Two of the preserved lateral line scales in reconstructed position showing their degree of overlap and expected orientation relative to the epidermis. In panels m, n: area of overlap with adjacent scale in the row shown in orange, area of overlap with scale in adjacent row shown in pink. Abbreviations: asp, anterior suprascalar pore; pip, posterior infrascalar pore; p, pore.

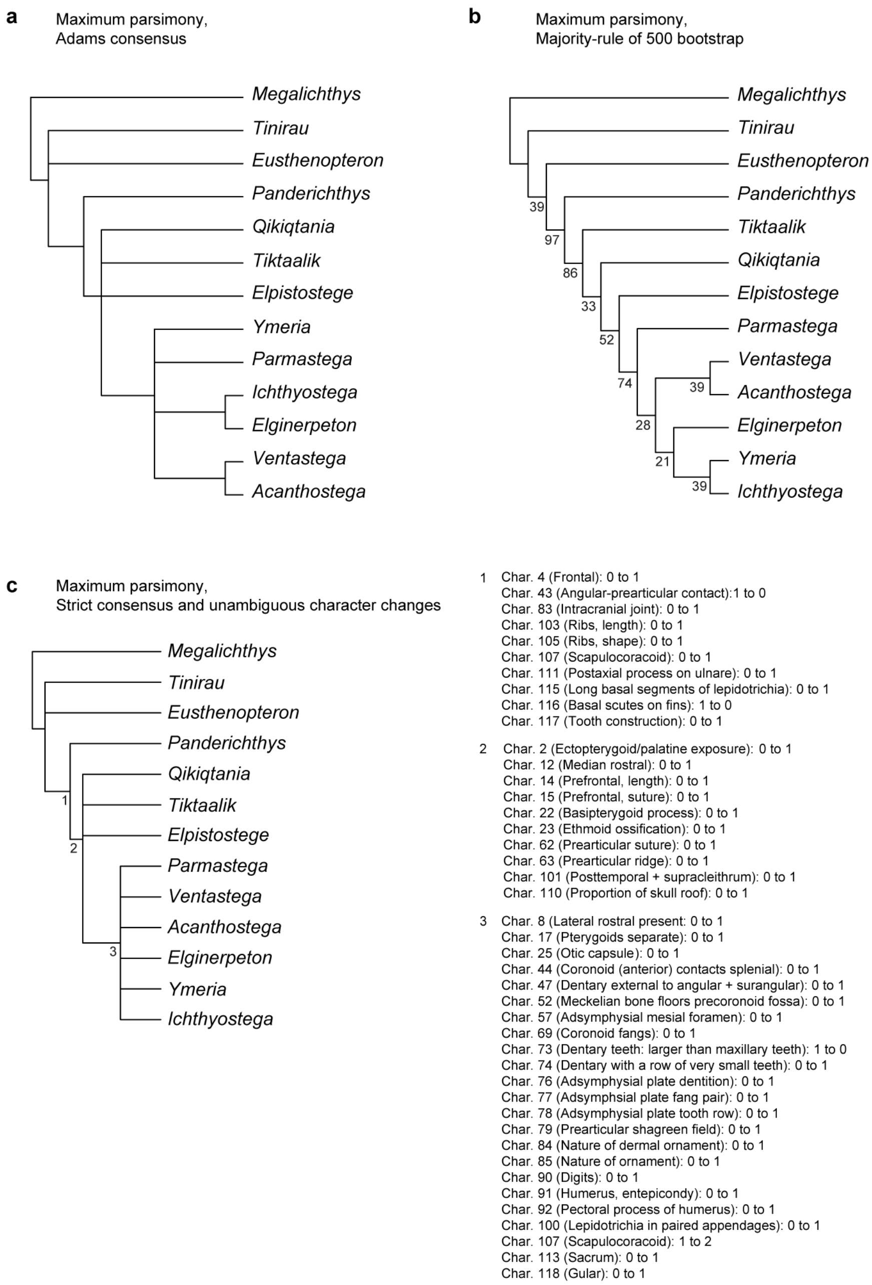

Extended Data Figure 5 | Expanded results of phylogenetic analyses.

(a) Adams consensus tree of maximum parsimony analyses. (b) Majority rule tree of maximum parsimony analyses with bootstrapping (500 replicates). In all panels, *Megalichthys* is plotted as the outgroup consistent with previous phylogenetic analyses of early tetrapods[9,23,25], although basal polytomies are recovered. (c) Unambiguous character changes recovered on the strict consensus tree using the command 'apolist' from PAUP*[38].

Supplementary Information for:

A New Elpistostegalian from the Late Devonian of Canadian Arctic

By T.A. Stewart, J.B. Lemberg, A. Daly, E.B. Daeschler, N. Shubin

This PDF file includes:

Supplementary Methods
Supplementary Discussion
Supplementary Table 1
Captions for Data S1 to S3
Captions for Videos S1 to S3
Supplementary References

Other Supplementary Materials for this manuscript include:

Supplementary Data 1 to 3
Supplementary Video 1 to 3

Supplementary Methods

Taxonomic sampling for phylogenetic analyses

These data are primarily based upon phylogenetic analyses of early tetrapods by Ahlberg and Clack[23], which included data for 10 of the 12 previously described taxa in this study (*Acanthostega*, *Elginerpeton*, *Elpistostege*, *Eusthenopteron*, *Ichthyostega*, *Panderichthys*, *Parmastega*, *Tiktaalik*, *Ventastega*, and *Ymeria*). This taxon set was expanded to include data for two additional tetrapodomorphs, *Megalichthys* and *Tinirau*, using the phylogenetic matrixes of Swartz[24] and Cloutier et al.[9].

Character coding

Characters 1-109 are from Ahlberg and Clack[23]. Data for *Megalichthys* and *Tinirau* were added for these characters by manually matching the coding of characters from Swartz[24] and Cloutier et al.[9] as noted in the character list. Coding for *Megalichthys* was confirmed by checking species-level coding in Clement et al.[36].

Cloutier *et* al.[9] presented a phylogenetic analysis of tetrapodomorphs and in that work reevaluated and updated a number of previously published character codings. If any character that they updated was included amongst characters 1-109, we adopted their changes, with one exception, character 90 (the presence or absence of digits). We code *E. watsoni* as ambiguous for this character. Where Cloutier et al.[9] changes were applied to the characters of the Ahlberg and Clack[23] matrix, it has been noted below as 'character changed' with reference and description given.

Characters 110-121 are from Cloutier et al.[9]. The Cloutier paper included data from 9 of the 12 previously described taxa in this study (*Acanthostega*, *Elpistostege*, *Eusthenopteron*, *Ichthyostega*, *Tiktaalik*, *Panderichthys, Ventastega*, *Megalichthys* and *Tinirau*). For those not included in their data set (*Elginerpeton*, *Parmastega*, and *Ymeria*), we referred to the literature to evaluate whether coding could be added. For all instances where additional data is included for these three taxa, it is noted below as 'coding added' with references given.

Characters 122-125, which focus on post-cranial anatomy, are new characters. All instances of data being included for these four characters is noted below as ‘coding added’ with references given.

Character list

The source of each character is noted at the end of the character description:
AC -Ahlberg and Clack 2020 (largely from Clack and Ahlberg[42] and [43]);
C - Cloutier et al 2020[9];
S - Swartz 2012[24].

1 Anterior tectal/septomaxilla: anterior tectal (external bone, dorsal to nostril): = 0, septomaxilla (external or internal bone, posterior to nostril) = 1, absent = 2 (AC1, C5, S84)

2 Ectopterygoid/palatine exposure: more or less confined to tooth row = 0, broad mesial exposure additional to tooth row = 1 (AC2, S76)

3 Ectopterygoid reaches subtemporal fossa: no = 0, yes = 1 (AC3, S79)

4 Frontal: absent = 0, present = 1 (AC4, C19, S113)

5 Intertemporal: present = 0, absent = 1 (AC5, C16, S118)

6 Jugal: does not extend anterior to orbit = 0, extends anterior to orbit = 1 (AC6, C51, S94)

7 Lacrimal: contributes to orbital margin = 0, excluded from margin = 1 (AC7, C53, S92)

8 Lateral rostral present: yes = 0, no = 1 (AC8, S85)

9 Maxilla makes interdigitating suture with vomer: no = 0, yes = 1 (AC9, S55)

10 Maxilla external contact with premaxilla: narrow contact point not interdigitated = 0, interdigitating suture = 1 (AC10, S54)

11 Maxilla extends behind level of posterior margin of orbit: yes = 0, no = 1 (AC11)

12 Median rostral: single = 0, paired = 1, absent = 2 (AC12, S86)

13 Opercular: present = 0, absent = 1 (AC13, C113, S139)

14 Prefrontal: twice as long as broad, or less = 0, three times as long as broad or more = 1 (AC14, S106)

15 Prefrontal: transverse anterior suture with tectal = 0, tapers to point anteriorly = 1 (AC15, S107)

16 Preopercular: present = 0, absent = 1 (AC16, ~C58, S138)

17 Pterygoids separate in midline = 0, meet in midline anterior to cultriform process = 1 (AC17, C71, S70)

18 Pterygoid quadrate ramus margin in subtemporal fossa: concave = 0, with some convex component = 1 (AC18, 71)

19 Vomers separated by parasphenoid > half length: yes = 0, no = 1 (AC19, ~C67)

20 Vomers excluded from margin of interpterygoid vacuity: yes = 0, no = 1 (AC20)

21 Vomers nearly as broad as long, or broader = 0, about twice as long as broad, or longer = 1 (AC21, C61, S57)

22 Basipterygoid process: not strongly projecting with concave anterior face = 0, strongly projecting with flat anterior face = 1 (AC22, S12)

23 Ethmoid: fully ossified = 0, partly or wholly unossified = 1 (AC23, S1)

24 Hypophysial region: solid side wall pierced by small foramina for pituitary vein and other vessels = 0, single large foramen = 1 (AC24, S13)

25 Otic capsule: lateral commissure bearing hyomandibular facets: present = 0, absent = 1 (AC25, S14)

26 Parasphenoid: does not overlap basioccipital = 0, overlaps basioccipital =1 (AC26, S68)

27 Parasphenoid: denticulated field: present = 0, absent = 1 (AC27, S66)

28 Sphenoid: fully ossified, terminating posteriorly in intracranial joint or fused to otoccipital = 0, separated from otoccipital by unossified gap = 1 (AC28)

29 Ectopterygoid fang pairs: present = 0, absent = 1 (AC29, ~C73, S80)

30 Ectopterygoid row (3+) of smaller teeth: present = 0, absent = 1 (AC30, S81)

31 Ectopterygoid / palatine shagreen field: absent = 0, present = 1 (AC31, S78)

32 Maxilla tooth number: > 40 = 0, 30-40 = 1, < 30 = 2 (AC32)

33 Palatine row of smaller teeth: present = 0, absent = 1 (AC33)

34 Pterygoid shagreen: dense = 0, a few discontinuous patches or absent = 1 (AC34, S73)

35 Premaxillary tooth proportions: all approximately same size = 0, posteriormost teeth at least twice height of anteriormost teeth = 1 (AC35, ~C187, S53)

36 Vomerine fang pairs: present = 0, absent = 1 (AC36, S58)

37 Vomerine fang pairs noticeably smaller than other palatal fang pairs: no = 0, yes = 1 (AC37, S59)

38 Vomer anterior wall forming posterior margin of palatal fossa bears tooth row meeting in midline: yes = 0, no = 1 (AC38, S61)

39 Vomerine row of small teeth: present = 0, absent = 1 (AC39, S60)

40 Vomerine shagreen field: absent = 0, present = 1 (AC40, S62)

41 Adductor fossa faces dorsally = 0, mesially = 1 (AC41)

42 Adductor crest: absent = 0, peak anterior to adductor fossa, dorsal margin of fossa concave = 1, peak above anterior part of adductor fossa, dorsal margin of fossa convex = 2 (AC42, S52)

43 Angular-prearticular contact: prearticular contacts angular edge to edge = 0, absent = 1, mesial lamina of angular sutures with prearticular = 2 (AC43, ~C91, S48)

44 Coronoid (anterior) contacts splenial: no = 0, yes = 1 (AC44, C89, S40)

45 Coronoid (posterior) posterodorsal process: no = 0, yes = 1 (AC45, S40)

46 Coronoid (posterior) posterodorsal process visible in lateral view: no = 0, yes = 1 (AC46, S43)

47 Dentary external to angular + surangular, with chamfered ventral edge and no interdigitations: no = 0, yes = 1 (AC47)

48 Dentary ventral edge: smooth continuous line = 0, abruptly tapering or ‘stepped’ margin = 1 (AC48, S27)

49 Mandibular sensory canal: present = 0, absent = 1 (AC49, S131)

50 Mandibular canal exposure: entirely enclosed, opens through lines of pores = 0, mostly enclosed, short sections of open grooves = 1, mostly open grooves, short sections opening through pores = 2, entirely open = 3 (AC50, S132)

51 Mandible: oral sulcus/surangular pit line: present = 0, absent = 1 (AC51, S133)

52 Meckelian bone floors precoronoid fossa: yes = 0, no = 1 (AC52)

53 Meckelian bone ossified in middle part of jaw: yes = 0, little or no ossification = 1 (AC53, ~C78)

54 Meckelian foramina/ fenestrae, dorsal margins formed by; Meckelian bone = 0, prearticular = 1, infradentary = 2 (AC54, S31)

55 Meckelian foramina/ fenestrae, height: much lower than adjacent prearticular = 0, equal to or greater than depth of adjacent prearticular = 1 (AC55, S32)

56 Adsymphysial lateral foramen present: no = 0, yes = 1 (Following Ahlberg and Clack 2020: the character follows a terminology change from "parasymphysial" to "adsymphysial.") (AC56, S20)

57 Adsymphysial mesial foramen present: no = 0, yes = 1 (AC57, C96, S21)

58 Postsplenial with mesial lamina: no = 0, yes = 1 (AC58, S30)

59 Postsplenial pit line present: yes = 0, no = 1 (AC59)

60 Postsplenial suture with prearticular present: no = 0, yes but interrupted by Meckelian foramina or fenestrae = 1, uninterrupted suture = 2 (AC60, C88, S29)

61 Prearticular sutures with surangular: no = 0, yes = 1 (AC61, S49)

62 Prearticular sutures with mesial lamina of splenial: no, mesial lamina of splenial absent = 0, yes = 1, no, mesial lamina of splenial separated from prearticular by postsplenial = 2 (AC62, C90)

63 Prearticular with longitudinal ridge below coronoids: no = 0, yes = 1 (AC63, C102)

64 Prearticular with mesially projecting flange on dorsal edge along posterior border of adductor fossa: no = 0, yes = 1 (AC64, S51)

65 Prearticular centre of radiation of striations: level with posterior end of posterior coronoid = 0, level with middle of adductor fossa = 1, level with posterior end of adductor fossa = 2 (AC65)

66 Splenial has free ventral flange: yes = 0, no = 1 (AC66)

67 Splenial, rearmost extension of mesial lamina: closer to anterior end of jaw than to adductor fossa = 0, equidistant = 1, closer to anterior margin of adductor fossa than to the anterior end of the jaw = 2 (AC67, ~C90)

68 Coronoids: at least one has fang pair recognizable because at least twice the height of coronoid teeth: yes = 0, no = 1 (AC68, ~C97, S36)

69 Coronoids: at least one has fangs recognizable because noticeably mesial to vertical lamina of bone and to all other teeth: yes = 0, no = 1 (AC69)

70 Coronoids: at least one has organized tooth row: yes = 0, no =1 (AC70, ~C98, S38)

71 Coronoids: at least one carries shagreen: no = 0, yes = 1 (AC71, S37)

72 Coronoids: size of teeth (excluding fangs) on anterior and middle coronoids relative to dentary tooth size: about the same = 0, half height or less = 1 (AC72, S39)

73 Dentary teeth: larger than maxillary teeth = 0, same size as maxillary teeth = 1, smaller than maxillary teeth = 2 (AC73, S23)

74 Dentary with a row of very small teeth or denticles lateral to tooth row: yes = 0, no = 1 (AC74, C87, S24)

75 Adsymphysial tooth plate: present = 0, absent = 1 (AC75, C93, ~S16)

76 Adsymphysial plate dentition: shagreen or irregular tooth field = 0, organized dentition aligned parallel to jaw margin = 1, no dentition = 2 (AC76, ~C95, S17)

77 Adsymphsial plate has fang pair: no = 0, yes = 1 (AC77, S18)

78 Adsymphysial plate has tooth row: no = 0, short tooth row, separated from coronoid tooth row by diastema = 1, long tooth row reaching coronoid = 2 (AC78, ~C95)

79 Prearticular shagreen field, distribution: gradually decreasing from dorsal to ventral = 0, well defined dorsal longitudinal band = 1, scattered patches or absent = 2 (AC79, S50)

80 Anterior palatal fenestra: single = 0, double = 1, absent = 2 (AC80, S74)

81 Dorsal fontanelle on snout: absent = 0, present = 1 (AC81, S87)

82 Interpterygoid vacuities: absent = 0, at least 2 x longer than wide = 1, < 2 x longer than wide = 2 (AC82, S75)

83 Intracranial joint: present in dermal skull roof = 0, absent = 1 (AC83, C25, S119)

84 Nature of dermal ornament: tuberculate = 0, fairly regular pit and ridge = 1, irregular = 2, absent or almost absent = 3 (AC84, S195)

85 Nature of ornament: ‘starbursts’ of radiating ornament on at least some bones: no = 0, yes = 1 (AC85, S196)

86 Keyhole-shaped orbits: absent = 0, present = 1 (AC86)

87 Anocleithrum: oblong with distinct anterior overlap area = 0, drop-shaped with no anterior overlap area = 1, absent = 2 (AC87, C188, S147)

88 Cleithrum: ornamented = 0, not ornamented = 1 (AC88, C126, S197)

89 Cleithrum, postbranchial lamina: present = 0, absent = 1 (AC89, S149)

90 Digits: absent = 0, present = 1 (AC90, C152, S178)

91 Humerus: narrow tapering entepicondyle = 0, square or parallelogram-shaped entepicondyle = 1 (AC91, ~C145)

92 Pectoral process of humerus: absent = 0, present = 1 (AC82, C146)

93 Proximal limb of oblique ridge of humerus: present, separated from anterior margin of humerus by prepectoral space = 0, absent, replaced by deltopectoral crest = 1 (AC93)

94 Latissimus dorsi attachment of humerus: diffuse ridged area = 0, distinct process = 1 (AC94)

95 Foramina piercing oblique ventral ridge of humerus: many = 0, one moderately large foramen in addition to entepicondylar foramen = 1, entepicondylar foramen is the only large opening, other foramina are tiny pinpricks or absent = 2 (AC95)

96 Ilium, iliac canal: absent = 0, present = 1 (AC96, S180)

97 Ilium, posterior process: oriented posterodorsally = 0, oriented approximately horizontally posteriorly = 1 (AC97, S188)

98 Interclavicle: small and concealed or absent = 0, large and exposed = 1 (AC98, ~C134, S158)

99 Interclavicle shape: ovoid = 0, kite-shaped = 1, with posterior stalk = 2 (AC99, C190, S159)

100 Lepidotrichia in paired appendages: present = 0, absent = 1 (AC100, C194)

101 Posttemporal + supracleithrum: present = 0, absent = 1 (C101, C124, S144+S145)

102 Radius and ulna: radius much longer than ulna = 0, approximately equal length = 1 (AC102, C193)

103 Ribs, trunk: no longer than diameter of intercentrum = 0, longer = 1 (AC103, C195, S183)

104 Ribs, trunk: all straight = 0, at least some curving ventrally = 1 (AC104, S184)

105 Ribs, trunk: all cylindrical = 0, some or all bear flanges from posterior margin which narrow distally = 1, some or all flare distally = 2 (AC105, C196, S185)

106 Scapular blade: absent = 0, small with narrow top = 1, large with broad top = 2 (AC106, ~C136, S153)

107 Scapulocoracoid: small and tripodal = 0, large plate pierced by large coracoid foramen = 1, very large plate without large coracoid foramen = 2 (AC107, ~C135)

108 Subscapular fossa: broad and shallow = 0, deeply impressed posteriorly = 1 (AC108)

109 Squamation: complete body covering of scales, all similar = 0, ventral armour of gastralia = 1 (AC109, S200)

110 Proportion of skull roof lying anterior to middle of orbits: <50% = 0, >=50% = 1 (C2)

111 Postaxial process on ulnare: present = 0, absent = 1 (C147)

112 Radius length: longer than humerus = 0, equal to or shorter than humerus = 1 (C149)

113 Sacrum: absent = 0, present = 1 (C159)

114 Scales: round = 0, rhombic = 1 (C162)

115 Long basal segments of lepidotrichia in pectoral fin: absent = 0, present = 1 (C164)

116 Basal scutes on fins: absent = 0, present = 1 (C165)

117 Tooth construction: simple or generalized polyplocodont = 0, labyrinthodont = 1 (C169)

118 Gular: present = 0, absent = 1 (C177)

119 Olecranon process on ulna: absent = 0, present = 1 (C182)

120 Number radials articulating on ulnare 0-2 radials = 0, greater than 2 radials = 1 (C199)

121 Tabular horn: absent = 0, present = 1 (C202)

122 Dorsal fins: two = 0, fewer than two = 1 (new character)

123 Anal fin: present = 0, absent = 1 (new character)

124 Asymmetry in pectoral fin hemitrichia: cross sectional area (CSA) of hemitricha differ by less than 2-fold = 0, CSA is 2-fold or greater = 1 (new character)

125 Relative girdle size: pectoral girdle significantly taller than pelvic girdle in lateral aspect = 0, girdles are approximately the same height = 1 (new character)

<u>Modified and new character codings</u>

Acanthostega gunnari (3 codings added)

Character 122 was coded ‘1’ according to Coates[37] (their Fig. 7).

Character 123 was coded ‘1’ according to Coates[37] (their Fig. 7).

Character 125 was coded ‘1’ according to Coates[37] (their Figs. 14, 18, 19, 31).

Elginerpeton pancheni (1 coding added)

Character 113 was coded ‘1’ according to Ahlberg[10] (their char. 32).

Elpistostege watsoni (21 characters changed, 2 codings added)

Character 13 was changed from '?' to '0' on the basis of Cloutier et al.[9] (their char. 113)

Character 19 was changed from '?' to '1', on the basis of Cloutier et al.[9] (their char. 64)

Character 21 was changed from '?' to '0' on the basis of Cloutier et al.[9] (their char. 61)

Character 29 was changed from '?' to '0' on the basis of Cloutier et al.[9] (their char. 73)

Character 35 was changed from '0' to '1' on the basis Cloutier et al.[9] (their char.187)

Character 53 was changed from '?' to '0' on the basis of Cloutier et al.[9] (their char. 78)

Character 62 was changed from '?' to '0' on the basis of Cloutier et al.[9] (their char. 90)

Character 68 was changed from '?' to '0' on the basis of Cloutier et al.[9] (their char. 97)

Character 74 was changed from '?' to '1' on the basis of Cloutier et al.[9] (their char. 87)

Character 75 was changed from '?' to '0' on the basis of Cloutier et al.[9] (their char. 93)

Character 87 was changed from '?' to '0' on the basis of Cloutier et al.[9] (their char. 188)

Character 88 was changed from '?' to '1' on the basis of Cloutier et al.[9] (their char. 126)

Character 91 was changed from '?' to '0' on the basis of Cloutier et al.[9] (their char. 145).

Character 98 was changed from '?' to '1' on the basis of Cloutier et al.[9] (their char. 134).

Character 99 was changed from '?' to '1' on the basis of Cloutier et al.[9] (their char. 190).

Character 100 was changed from '?' to '0' on the basis of Cloutier et al.[9] (their char. 194).

Character 101 was changed from '?' to '1' on the basis of Cloutier et al.[9] (their char. 124).

Character 102 was changed from '?' to '0' on the basis of Cloutier et al.[9] (their char. 193).

Character 103 was changed from '?' to '0/1' on the basis of Cloutier et al.[9] (their char. 195).

Character 104 was coded as "?". Although Cloutier et al.[9] describe the pectoral fin of *E. watsoni* as possessing two digits, we regard this as uncertain. There are several reasons for this caution: (i) The position of the elements identified as the digits appears to be anterior to the primary axis of the fin, rather than positioned as a terminal series distal to the mesomeric axis. (ii) Multiple reconstructions are presented for the dataset that differ in the number, position, and geometry of the distal endoskeletal elements (their Fig. 3 c,d)[9]. (iii) The morphology of the elements is unusual for phalanges. Specifically, the anterior series has a distal phalanx with a proximal articular surface several times wider than the articular surface of its more proximal counterpart. The posterior series has a proximal phalanx with a post-axial flange that extends beyond the joint to nearly half the length of the more distal phalanx. To our knowledge, both patterns are unprecedented among digits. Given these matters of position, variable reconstruction, and unusual morphology, we regard the hypothesis that *E. watsoni* possessed digits as a valid one worthy of continued analysis; hence, the uncertainty in the coding.

Character 105 was changed from '?' to '1' on the basis of Cloutier et al.[9] (their char. 196).

Character 122 was coded ‘1’ on the basis of Cloutier et al.[9] (their Fig. 1).

Character 123 was coded ‘0’ on the basis of Cloutier et al.[9] (their Fig. 1).

Eusthenopteron foordi (4 codings added)

Character 122 was coded ‘0’ on the basis of Andrews and Westoll[28] (their Fig. 23).

Character 123 was coded ‘0’ on the basis of Andrews and Westoll[28] (their Fig. 23).

Character 124 was coded ‘0’ on the basis of Stewart et al.[7] (their Fig. 5).

Character 125 was coded ‘0’ on the basis of Andrews and Westoll[28] (their Fig. 23).

Ichthyostega (3 codings added)

Character 122 was coded ‘0’ on the basis of Ahlberg et al.[44] (their Fig. 1).

Character 123 was coded ‘0’ on the basis of Ahlberg et al.[44] (their Fig. 1).

Character 125 was coded ‘0’ on the basis of Ahlberg et al.[44] (their Fig. 1).

Megalichthys (9 codings changed, 2 codings added)

Character 53 was changed from ‘?’ to ‘0’ on the basis of Cloutier et al.[9] (their char. 78)

Character 62 was changed from ‘?’ to ‘0’ on the basis of Cloutier et al.[9] (their char. 90)

Character 63 was changed from ‘?’ to ‘0’ on the basis of Cloutier et al.[9] (their char. 102)

Character 91 was changed from ‘?’ to ‘0’ on the basis of Cloutier et al.[9] (their char. 145)

Character 92 was changed from ‘?’ to ‘0’ on the basis of Cloutier et al.[9] (their char. 146)

Character 100 was changed from ‘?’ to ‘0’ on the basis of Cloutier et al.[9] (their char. 194)

Character 101 was changed from ‘?’ to ‘0’ on the basis of Cloutier et al.[9] (their char. 124)

Character 102 was changed from ‘?’ to ‘0’ on the basis of Cloutier et al.[9] (their char. 193)

Character 107 was changed from ‘?’ to ‘0’ on the basis of Cloutier et al.[9] (their char. 135)

Character 122 was coded ‘1’ according to Wellburn[45] (their Plate XIII).

Character 123 was coded ‘1’ according to Wellburn[45] (their Plate XIII).

Panderichthys pancheni (3 characters changed)

Character 6 was changed from '0' to '0/1' on the basis of Cloutier et al.[9] (their char. 51)

Character 35 was changed from '0' to '1' on the basis of Cloutier et al.[9] (their char. 187)

Character 99 was changed from '?' to '0' on the basis of Cloutier et al.[9] (their char. 190)

Parmastega aelidae (2 codings added)

Character 118 was coded as '1' on the basis of Beznosov et al.[46] (their discussion section). Character 121 was added as '1' on the basis of Beznosov et al.[46] (their Fig. 1 G).

Tiktaalik roseae (45 characters changed, 3 codings added)

We corrected and updated character codings for ~35% of the *T. roseae* data. These are based upon studies of the cranium[8,47], pectoral girdle and fins[7,48], pelvic girdle and fin[6]. When the anatomy has been figured, we refer to the pertinent manuscript and figure. If the character has not been figured but can be observed in a publicly available data set, we refer to that, providing a DOI of the dataset.

Character 1 was changed from '?' to '0' on the basis of Lemberg et al.[8], which describes the presence of an anterior tectal. They are diagnosable in CT scans of specimens NUFV 108, NUFV 110, and NUFV 149 and lie immediately anterior to the prefrontal and are overlapped slightly by the anterior tip of the lacrimal (data available here https://doi.org/10.17602/M2/M168208).

Character 2 was changed from '0' to '1' on the basis of Lemberg et al.[8], which shows the feature on specimen NUFV 108 (their Fig. 2 A).

Character 3 was changed from '?' to '1' on the basis of Lemberg et al.[8], which shows the feature on specimen NUFV 108 (their Fig. 2 A, B).

Character 5 was changed from '1' to '0' on the basis of Lemberg et al.[8], which shows the feature on specimen NUFV 108 (their Fig. 2 B).

Character 7 was changed from '?' to '1' on the basis of Lemberg et al.[8], which shows the feature on specimens NUFV 108 and NUFV 110 (their Figs. 1, 2B).

Character 8 was changed from '?' to '0' on the basis of Lemberg et al.[8], which presents CT data for specimens NUFV 108, NUFV 110 and NUFV 149 that show the presence of the lateral rostral (data available here https://doi.org/10.17602/M2/M168208).

Character 9 was changed from '?' to '0' on the basis of Lemberg et al.[8], which shows the feature on specimen NUFV 108 (their Fig. 2 A).

Character 20 was changed from '?' to '-' on the basis of CT data presented in Lemberg et al.[8] (data available here https://doi.org/10.17602/M2/M168208).

Character 21 was changed from '?' to '0' on the basis of Lemberg et al.[8], which shows the feature on specimen NUFV 108 (their Fig. 2 A).

Character 22 was changed from '0' to '1' on the basis of Lemberg et al.[8], which shows the feature on specimen NUFV 108 (their Fig. 2 A, B; Fig. 3A).

Character 23 was changed from '0' to '1' on the basis of Lemberg et al.[8], which presents CT data that show the ethmoid to be partially ossified. This is diagnosable in the scans, as the ethmoid shows a cortex of higher density ossification with more medial portions less fully ossified. These medial portions are also less ossified than either the lower jaw or vomer. This is observed most clearly in specimen NUFV 149 (data available here https://doi.org/10.17602/M2/M168955, https://doi.org/10.17602/M2/M168954)

Character 24 was changed from '?' to '0' on the basis of Downs et al.[47] (Fig 2). CT data presented in Lemberg et al.[8] for specimens NUFV 108, NUFV 110, and NUFV 149 support this diagnosis.

Character 27 was changed from '?' to '0' on the basis of Lemberg et al.[8], which shows the feature on specimen NUFV 108 (their Fig. 2 A).

Character 29 was changed from '?' to '0' on the basis of Lemberg et al.[8], which shows the feature on specimen NUFV 108 (their Fig. 2 A).

Character 30 was changed from '?' to '0' on the basis of Lemberg et al.[8], which shows the feature on specimen NUFV 108 (their Fig. 2 A) .

Character 31 was changed from '?' to '0' on the basis of Lemberg et al.[8], which shows the feature on specimen NUFV 108 (their Fig. 2 A).

Character 33 was changed from '?' to '0' on the basis of Lemberg et al.[8], which shows the feature on specimen NUFV 108 (their Fig. 2 A).

Character 36 was changed from '?' to '0' on the basis of Lemberg et al.[8], which shows the feature on specimen NUFV 108 (their Fig. 2 A).

Character 37 was changed from '?' to '0' on the basis of Lemberg et al.[8], which shows the feature on specimen NUFV 108 (their Fig. 2 A).

Character 38 was changed from '?' to '0' on the basis of Lemberg et al.[8], which shows the feature on specimen NUFV 108 (their Fig. 2 A).

Character 39 was changed from '?' to '0' on the basis of Lemberg et al.[8], which presents CT data for specimen NUFV 108 (their Fig. 2 A).

Character 40 was changed from '?' to '0' on the basis of Lemberg et al.[8], which presents CT data for specimen NUFV 108 (their Fig. 2 A).

Character 43 was changed from '0' to '0/1' on the basis of CT data of specimen NUFV 108, which was published in association with Lemberg et al.[8] (data available here: https://doi.org/10.17602/M2/M168208)

Character 51 was changed from '?' to '0' on the basis of CT data of specimen NUFV 108, which was published in association with Lemberg et al.[8] (data available here: https://doi.org/10.17602/M2/M168208)

Character 53 was changed from '0' to '0/1' on the basis of CT data of specimen NUFV 108, which was published in association with Lemberg et al.[8] (data available here: https://doi.org/10.17602/M2/M168208)

Character 54 was changed from '?' to '0' on the basis of CT data of specimen NUFV 108, which was published in association with Lemberg et al.[8] (data available here: https://doi.org/10.17602/M2/M168208)

Character 59 was changed from '?' to '0' on the basis of CT data of specimen NUFV 108, which was published in association with Lemberg et al.[8] (data available here: https://doi.org/10.17602/M2/M168208)

Character 60 was changed from '?' to '0' on the basis of CT data of specimen NUFV 108, which was published in association with Lemberg et al.[8] (data available here: https://doi.org/10.17602/M2/M168208)

Character 62 was changed from '0' to '1' on the basis of CT data of specimen NUFV 108, which was published in association with Lemberg et al.[8] (data available here: https://doi.org/10.17602/M2/M168208)

Character 63 was changed from '0' to '1' on the basis of CT data of specimen NUFV 108, which was published in association with Lemberg et al.[8] (data available here: https://doi.org/10.17602/M2/M168208)

Character 65 was changed from '?' to '-' on the basis of CT data of specimen NUFV 108, which was published in association with Lemberg et al.[8] (data available here: https://doi.org/10.17602/M2/M168208)

Character 66 was changed from '?' to '0' on the basis of CT data of specimen NUFV 108, which was published in association with Lemberg et al.[8] (data available here: https://doi.org/10.17602/M2/M168208)

Character 67 was changed from '?' to '0' on the basis of CT data of specimen NUFV 108, which was published in association with Lemberg et al.[8] (data available here: https://doi.org/10.17602/M2/M168208)

Character 73 was changed from '?' to '1' on the basis of CT data of specimen NUFV 108, which was published in association with Lemberg et al.[8] (data available here: https://doi.org/10.17602/M2/M168208)

Character 74 was changed from '1' to '0' on the basis of CT data of specimen NUFV 108, which was published in association with Lemberg et al.[8] (data available here: https://doi.org/10.17602/M2/M168208)

Character 76 was changed from '?' to '0' on the basis of Lemberg et al.[8], which presents CT data for specimen NUFV 108 (their Fig. 2 A).

Character 77 was changed from '?' to '0' on the basis of CT data of specimen NUFV 108, which was published in association with Lemberg et al.[8] (data available here: https://doi.org/10.17602/M2/M168208)

Character 79 was changed from '0' to '0/1' on the basis of CT data of specimen NUFV 108, which was published in association with Lemberg et al.[8] (data available here: https://doi.org/10.17602/M2/M168208)

Character 80 was changed from '?' to '0' on the basis of CT data of specimen NUFV 108, which was published in association with Lemberg et al.[8] (data available here: https://doi.org/10.17602/M2/M168208)

Character 95 was changed from '?' to '0' on the basis of Shubin et al.[5], which describes the humerus of *Tiktaalik* and shows the feature on specimen NUFV 109 (their Fig. 2). Stewart *et* al.[7], also presents CT data of the humerus of specimen NUFV 110 (their Fig 3, Movie S3).

Character 99 was changed from '?' to '0' on the basis of Shubin et al.[48], which describe the interclavicles of specimen NUFV 109 (their Fig. 4.6).

Character 104 was changed from '0' to '1' on the basis of the specimen NUFV 108, which shows ventralward curvature of the posterior-most rib preserved on the left side.

Character 105 was changed from '?' to '1' on the basis of Daeschler et al.[4], which describes ribs in specimen NUFV 108 (their Figs. 3C, 6). Additional photographs of the ribs of NUFV 108 are provided in Shubin et al.[6] (their Fig. 2).

Character 108 was changed from '?' to '0' on the basis of Shubin et al.[5], which describes the shoulder girdle of specimen NUFV 112 (their Figs. 3, 5b).

Character 109 was changed from '?' to '0' on the basis of Daeschler et al.[4] (their Fig. 2) and Shubin et al.[6] (their Fig. 2), which show scalation on the dorsal and ventral surfaces, respectively, of specimen NUFV 108.

Character 122 was coded as ‘1’ on the basis of examination of the specimen NUFV 108. The specimen preserves the dorsal series of scales in position from posterior to the cranium to the pelvis. In other tetrapodomorphs where two dorsal fins are present (e.g., *Eusthenopteron*) the anterior dorsal fin is positioned anterior to or at the level of the pelvis. Therefore, we diagnose a condition of not having two dorsal fins. Whether a single dorsal fin posterior to the pelvis was present is unclear.

Character 123 was coded as ‘1’ on the basis of examination of the specimen NUFV 108, which preserves the axial skeleton and ventral scales posterior to the pelvis and does not preserve an anal fin.

Character 124 was coded as ‘1’ on the basis of Stewart et al.[7], which describes the anatomy of pectoral fin hemitrichia in specimens NUFV 108 and NUFV 109 (their Figs. 3, 5, S6).

Character 125 was coded as ‘1’ on the basis of Shubin et al.[6], which describes the right pelvis of specimen NUFV 108 (their Figs. 3, 5).

Tinirau clackae (6 character changed, 2 codings added)

Character 6 was changed from '0' to '?' on the basis of Cloutier et al.[9] (their char. 51).

Character 53 was changed from ‘?’ to ‘1’ on the basis of Cloutier et al.[9] (their char. 78)

Character 62 was changed from ‘?’ to ‘0’ on the basis of Cloutier et al.[9] (their char. 90)

Character 91 was changed from ‘?’ to ‘0’ on the basis of Cloutier et al.[9] (their char. 145)

Character 100 was changed from ‘?’ to ‘0’ on the basis of Cloutier et al.[9] (their char. 194)

Character 102 was changed from ‘?’ to ‘0’ on the basis of Cloutier et al.[9] (their char. 193)

Character 123 was coded ‘1’ according to Swartz[24] (their Fig. 2).

Character 125 was coded ‘1’ according to Swartz[24] (their Fig 2).

Ventastega curonica (2 characters changed)

Character 13 was changed from '1' to '?' on the basis of Cloutier et al.[9] (their char. 113).

Character 21 was changed from '0' to '?' on the basis of Cloutier et al.[9] (their char. 61).

Supplementary Discussion

Size and body proportions

Figure 1 c shows NUFV 137 framed by a line drawing of a body. This drawing is based upon the proportions of *E. watsoni* (specimen MHNM 06-2067[9]) and scaled to the length of the lower jaw. Assuming these proportions, NUFV 137 measures approximately 75 cm standard length (from tip of the snout to the end of the last vertebrae).

Taphonomy

The pectoral fin shows postmortem displacement of several elements. In other finned tetrapodomorphs, lepidotrichia of the pectoral fin do not extend further proximally than to the base of the radius. However, in NUFV 137 lepidotrichia are positioned more proximally, overlapping the humerus on the ventral side, indicating that the fin web has been shifted relative to the proximal endoskeleton.

The intermedium is also displaced—as preserved, it contacts the humerus proximally and is positioned slightly dorsal to the radius. Although it is difficult to discern the natural boundaries of the intermedium and the radius from cross sections of CT data alone, we estimated the boundaries of this element on the basis of external geometry of the fully segmented endoskeleton. The posterior boundary of the intermedium is clearly demarcated by the ulna, which is significantly deeper than the adjacent intermedium. The anterior boundary of the intermedium is more challenging to determine, as there is not an abrupt change in depth to denote the posterior margin of the radius. Because the distal extent of the intermedium is estimated to reach the distal terminus of the ulna in its preserved position, we approximated the anterior boundary of the intermedium so that the there was a gradual curve from the proximo-anterior corner to the postero-distal corner. On the basis of the geometry of the proximal articular surfaces of the radius and ulna, we demarcate the proximal width of the intermedium (Fig. 3 c). This width is consistent with the space available for articulation on the ulna (Fig. 3 d). We note that these reconstructions do not affect the diagnosis, phylogenetic analysis, or interpretations of *Q. wakei.*

The humerus is narrow in the dorsoventral direction, raising the question of the extent to which its morphology reflects dorsoventral compression. The posterodistal portion of the humerus that articulates with the ulna is of a similar depth as the proximal articular surface of the ulna (Video S3), indicating that among the endoskeletal elements, the humerus is not disproportionately flattened. Given that the proximal articular surfaces of the radius and ulna (Fig. 3 c) are similar in their shape to other exceptionally three-dimensionally preserved tetrapodomorph humeri (e.g., *Sauripterus talori*[7,49] and *T. roseae*[7]), we argue that the much of the narrowness of the humerus reflects a gracile phenotype in life. We additionally note that such compression is unlikely to impact diagnosis of phylogenetic characters that are based on the fin. For example, both *P. rhombolepis* and *T. roseae* are known from multiple specimens showing degrees of dorsoventral compression (e.g., specimens GIT434-1[2] and PIN 3547-19[3] for *P. rhombolepis*, and specimens NUFV 109[5] and NUFV 110[7] for *T. roseae*). For both taxa, even in the compressed specimens features like ectepicondyle, humeral ridge and its associated foramina are preserved[2,3,5,7]. Similarly, the *E. watsoni* specimen MHNM 06-2067[9] is described as compressed, and its humerus preserves features that are absent in *Q. wakei*.

Table S1. µCT scanning parameters.

Each row represents an individually scanned element with voltage, current, filter, and resolution provided. All scans were collected using a GE Phoenix v|tome|x 240 kv/180kv scanner. All data are deposited on MorphoSource (https://www.morphosource.org/projects/000375542). Panel labels for each element correspond to photos in Extended Data Fig. 2.

panel	element	tube	voltage	current	filter	voxel size	DOI
a	symphysis	180	160 kV	60 µA	0.12 mm Cu	31.754 µm	https://doi.org/10.17602/M2/M407134
b	middle section of left jaws (lower and upper)	180	90 kV	108 µA	none	9.708 µm	https://doi.org/10.17602/M2/M408179
c	fragmentary portions of dermopalatine, ectopterygoid, middle coronoid and dentary	180	90 kV	200 µA	none	9.098 µm	https://doi.org/10.17602/M2/M408195
d	left principal gular and ceratohyal	180	90 kV	200 µA	none	18.337 µm	https://doi.org/10.17602/M2/M408201
e	fragmentary portions of palate and lower jaw	180	90 kV	105 µA	none	9.515 µm	https://doi.org/10.17602/M2/M408209
f	small posterior jaw fragment	180	90 kV	200 µA	none	9.265 µm	https://doi.org/10.17602/M2/M408289
g	fragment of the marginal tooth row	240	150 kV	350 µA	0.56 mm Sn	62.081 µm	https://doi.org/10.17602/M2/M408295
h	left pectoral fin	240	90 kV	380 µA	0.25 mm Cu	43.287 µm	Awaiting DOI assignment
i	fragment containing fin rays and scales	180	90 kV	200 µA	none	21.555 µm	https://doi.org/10.17602/M2/M408306

j	small, crushed endochondral element	180	90 kV	200 µA	none	14.037 µm	https://doi.org/10.17602/M2/M410039
k	small vascularized endochondral element	180	90 kV	200 µA	none	8.342 µm	https://doi.org/10.17602/M2/M410051
l	small section of dorsal midline scales	240	100 kV	350 µA	none	35.096 µm	https://doi.org/10.17602/M2/M408312
m	small section of left lateral line scales	180	90 kV	115 µA	none	10.831 µm	https://doi.org/10.17602/M2/M408318
n	large section of left flank scales	240	100 kV	400 µA	none	59.004 µm	https://doi.org/10.17602/M2/M408324

Supplementary Data 1. Image Files

A zipped file containing high-resolution images of all figures.

Supplementary Data 2. PAUP* files.

A zipped file that contains a PAUP* executable file, each of the most-parsimonious trees, and consensus trees (strict, Adams and 50% majority-rule).

Supplementary Data 3. MrBayes files.

A zipped file that contains a MrBayes executable file, screen log, and majority-rule consensus tree.

Supplementary Video 1.

Volumetric rendering of all NUFV 137 elements in approximate positions.

Supplementary Video 1.

Volumetric rendering of the feeding apparatus of NUFV 137.

Supplementary Video 2.

Volumetric rendeslring of the pectoral fin of NUFV 137.

Supplementary References

42 Clack, J. A. & Ahlberg, P. E. in *Recent Advances in the Origin and Radiation of Vertebrates* (eds G. Arratia, M.V.H. Wilson, & R. Cloutier) (Verlag Dr. Friedrich Pfeil, 2004).

43 Chen, D. *et al.* A partial lower jaw of a tetrapod from "Romer's Gap". *Earth and Environmental Science Transactions of the Royal Society of Edinburgh* **108**, 55-65, doi:10.1017/S1755691018000099 (2017).

44 Ahlberg, P. E., Clack, J. A. & Blom, H. The axial skeleton of the Devonian tetrapod *Ichthyostega*. *Nature* **437**, 137-140, doi:http://www.nature.com/nature/journal/v437/n7055/suppinfo/nature03893_S1.html (2005).

45 Wellburn, E. D. On the Genus *Megalichthys*, Agassiz: Its History, Systematic Position, and Structure. *Proceedings of the Yorkshire Geological Society* **14**, 52–71 (1900).

46 Beznosov, P. A., Clack, J. A., Lukševičs, E., Ruta, M. & Ahlberg, P. E. Morphology of the earliest reconstructable tetrapod *Parmastega aelidae*. *Nature* **574**, 527-531, doi:10.1038/s41586-019-1636-y (2019).

47 Downs, J. P., Daeschler, E. B., Jenkins, F. A. & Shubin, N. H. The cranial endoskeleton of *Tiktaalik roseae*. *Nature* **455**, 925-929, doi:10.1038/nature07189 (2008).

48 Shubin, N. H., Daeschler, E. B. & Jenkins, F. A. in *Great Transformations in Vertebrate Evolution* (eds K.P. Dial, N.H. Shubin, & E.L. Brainerd) 63-76 (The University of Chicago Press, 2015).

49 Davis, M. C., Shubin, N. & Daeschler, E. B. A new specimen of *Sauripterus taylori* (Sarcopterygii, Osteichthyes) from the Famennian Catskill Formation of North America. *Journal of Vertebrate Paleontology* **24**, 26-40, doi:10.1671/1920-3 (2004).